Paleontología Mexicana
Volumen 7, núm. 1, 2018, p. 23 – 56

Cambrian oncolites from San José de Gracia, Sonora, Mexico

Hugo Beraldi-Campesi[a,*], Francisco Cuen-Romero[b], Blanca E. Buitrón-Sánchez[c]

[a] Sociedad Mexicana de Astrobiologia-SOMA. Ciudad Universitaria, Coyoacán, C.P. 04510, Ciudad de México, México.
[b] Universidad de Sonora, División de Ciencias Exactas y Naturales, Departamento de Geología. Blvd. Luis Encinas y Rosales, C.P. 83000, Hermosillo, Sonora.
[c] Instituto de Geología, Universidad Nacional Autónoma de México. Ciudad Universitaria, Coyoacán, C.P. 04510, Ciudad de México, México.

[*] hberaldi@gmail.com

Abstract

Recently discovered oncolites from a Lower Cambrian locality in San José de Gracia (SJG), Sonora (Mexico), illustrate the wide geographic distribution that they had in this part of Laurentia some 515–510 Ma ago. They are exceptionally large (~44 mm) in comparison to other marine forms of the North American Cambrian Carbonate Bank, but similar in their overall morphology and depositional environment. Their association with abundant biomorphs, especially indigenous filamentous structures with the curvature and spatial arrangement that fit the minimum criteria for biogenicity, supports their biological origin. Key morphological features include laminated growth in at least a portion of the oncolite, subspherical shape with internal porosity, and a nucleated habit on skeletal debris (mollusk shells) and mud concretions. The similarity of SJG oncolites with others from Cambrian outcrops separated today by hundreds of kilometers, suggests that massive microbially-driven, shallow marine ecosystems existed in western Laurentia during this time. This speaks of the impact that microbes had in shaping marine sediments, and the global primary productivity and carbon cycle during early stages of the Phanerozoic.

Keywords: oncolites, Paleoecology, Geobiology, microbialites, sedimentary biostructures.

Resumen

Oncolitos descubiertos recientemente en una localidad del Cámbrico Temprano en San José de Gracia (SJG), Sonora (México), ilustran la amplia distribución que éstos tuvieron en esta parte de Laurentia hace unos 515–510 Ma. Son excepcionalmente grandes (~44 mm) en comparación con otras formas marinas del Banco de Carbonato del Cámbrico de Norte América, pero similares en morfología y ambiente de depósito. Su asociación con abundantes biomorfos, especialmente estructuras filamentosas con la curvatura y arreglo espacial que demuestran su biogenicidad, apoyan su origen biológico. Características morfológicas clave incluyen su crecimiento laminado al menos en alguna porción del oncolito, su forma sub-esférica con porosidad interna, y que están nucleados por fragmentos esqueletales (conchas de molusco) y concreciones pelíticas. La similitud de los oncolitos de SJG con otros de localidades que hoy se encuentran a cientos de kilómetros de distancia, sugiere que en esta parte de Laurentia existieron ecosistemas microbianos masivos en aguas someras en ese tiempo. Eso habla del impacto que tuvieron los microbios en la estructuración de los sedimentos, así como en la productividad primaria global y el ciclo del Carbono durante el Fanerozoico Temprano.

Palabras clave: oncolites, Paleoecología, Paleobiología, microbialitas, bioestructuras sedimentarias.

1. Introduction

1.1. A note on paleontological terminology

Although the terms 'oncolite' and ‘oncoid’ have been used interchangeably, they have different meanings. ‘Oncolite’ implies biogenicity while ‘oncoid’ refers to semispherical and layered sedimentary structures, regardless of origin (Flügel, 2004, p 123). In this contribution we use 'oncolite' to refer to microbially-mediated, individual, chemical sedimentary structures that are subspherical, concentrically laminated (at least to some degree), and unattached to the substrate. This usage is consistent with the use of the term 'stromatolite', a widely recognized type of microbialite. Likewise, we may refer to 'oncolitic limestone', 'oncolitic pavement', 'oncolitic conglomerate' as rocks bearing oncolites or simply 'oncolites' as a group of oncolites.

Oncolites have been mistakenly called 'calcareous algae', 'algal balls' or 'algal biscuits', or referred to the genus '*Girvanella*' in the literature. The term 'calcareous algae' refers to eukaryotic algae that precipitate carbonate on their surfaces (teguments), that is not necessarily microbially-driven nor concentrically laminated. 'Algal balls' can be regarded as rhodoliths, which are produced by eukaryotic red algae and where tegumentary features can be seen. *Girvanella* refers to tubular microfossils usually related to cyanobacteria (Riding, 1975) and not sedimentary structures. Lastly, 'algal biscuit' is a local term coined before 1960 to refer to oncolites. Other oncolites can even be built by foraminifers and metazoans (Rider and Enrico, 1979; Balson and Taylor 1982; Hillmer *et al*., 1996; Scholz, 2000). Therefore, in the strict sense of the term 'microbialite' (chemical sedimentary structure mediated by microbes), oncolites built by animals and centimetric algae must be differentiated from those built mainly by bacteria. If microbial oncolites are 'microbialites', eukaryotic types could be termed 'macrobialites'.

In coastal and fluvial environments, mid- to high-energy currents overturn millimeter-sized particles that gradually grow encrusted by mineral precipitates (typically calcium carbonate; Peryt, 1981), to finally form a bigger semi-spherical structure that results in an oncolite that is > 5 mm to several cm in diameter. Similar, but smaller structures (< 2 mm) are called 'ooids' and are prevalent since the Archean (Reimer, 1975). Note that much of the shape of oncolites is due to the shape of their nuclear materials. In a crater lake in Mexico one of the authors (HBC) has studied oncolites that range from 5 mm to meter-long ‘tree’ trunks that have been encrusted with carbonates the same way, and where a green layer of microbes can be seen ~1 mm below the surface. In fact, significantly larger oncolites could occur in fluvial and lacustrine environments (Winsborough *et al*., 1994; Wade and Garcia-Pichel, 2003; Pickford *et al*., 2009) in comparison to those of marine environments.

1.2. Oncolites in Mexico

Fossil oncolites have been poorly studied in Mexico, although examples are known from Cambrian (Cooper *et al*., 1952) and upper Paleozoic (Buitrón-Sánchez *et al*., 2012) strata, and also the Holocene (Winsborough *et al*., 1994; Wade and Garcia-Pichel, 2003). These investigations have approached the study of oncolites and other microbialites from a variety of different perspectives including paleontology, stratigraphy, ecology, and DNA surveys, and have increased our knowledge about their occurrence, morphology, ecology, and environmental requirements for development.

The oldest reported oncolites from Mexico come from Lower Cambrian rocks of the Caborca region in Sonora (Cooper *et al*., 1952; Nardin *et al*., 2009). Recently discovered Lower Cambrian oncolites in San José de Gracia (SJG), near the city of Hermosillo (Figure 1), widen the extension of those from northern Caborca and represent important repositories of the history of microbialites in Mexico. They are also useful paleoenvironmental indicators whenever associated with index fossils and lithological successions. Moreover, this type of oncolites could be useful markers to correlate distant Cambrian outcrops, which is the case for Sonora and western North America. However, this is only true when index fossils and the overall lithology are also considered.

2. Cambrian strata in Sonora

Cambrian outcrops in Mexico typically display igneous and metamorphic rocks, while sedimentary rocks are rare (Figure1A). Sedimentary units of Cambrian age are known only from Sonora. King (1940) studied Cambrian to Ordovician rocks in the Cobachi region, while Cooper *et al*. (1952) worked on the stratigraphy and fossil content of marine deposits of the Caborca region, providing the first descriptions of archaeocyathids, brachiopods, trilobites, and oncolites (then referred to *Girvanella*). Baldis and Bordonaro (1981) discussed the correlation between Cambrian trilobites from Sonora with those from the Precordillera in Argentina, giving the first hints of biostratigraphic correlations at the continental scale for Cambrian rocks in Mexico. Stewart *et al*. (1984, 2002) further correlated Cambrian units of Sonora and Western USA, and compiled a stratigraphic and paleontological report, where they mention the presence of oncolites in the Buelna, Cerro Prieto, and Arrojos formations, some of which have been found in SJG (Cuen *et al*., 2016). McMenamin (1985, 1987) contributed to the biostratigraphy of Cambrian trilobites in the region of Puerto Blanco (Sonora), which helped to refine ages based on index fossils of the *Nevadella*, *Olenellus*, and *Bonnia* types. Rivera-Carranco (1988a, b) defined the paleoenvironmental onditions of various Cambrian sedimentary units of Sonora, and Almazán-

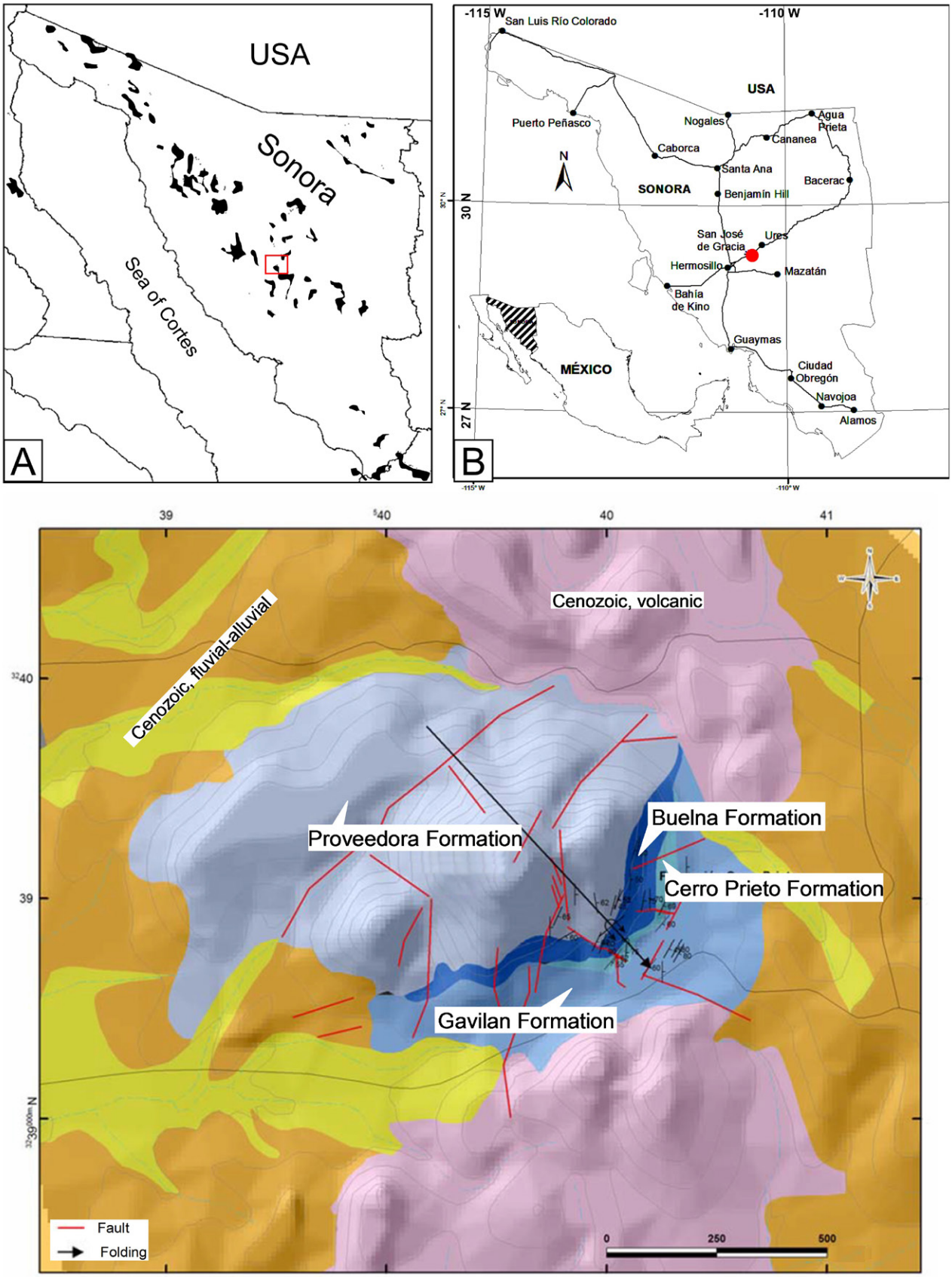

Figure 1. A. Map of Cambrian outcrops (shaded areas) in Northern Mexico. Most of them are volcanogenic. Outcrop extension was exaggerated to achieve visual scale. The box indicates the location of San José de Gracia (SJG). B. Location of the Chihuarruita Hill in SJG. C. Geologic map of the Chihuarruita Hill, approximately 2.5 km East of San José de Gracia, Sonora, Mexico. Oncolites studied here belong to the Buelna Formation.

Vázquez (1989) wrote about the Cambrian-Ordovician outcrops in the Arivechi region, where oncolites have been found but not studied. Later, Riva and Ketner (1989) and Debrenne *et al*. (1989) provided new descriptions of Cambrian and Ordovician graptolites and archaeocyathids from the Caborca region, further refining the age and biostratigraphy of those rocks. Nardin *et al*. (2009) described the eocrinoids of Lower to Middle Cambrian of SJG, which was a pioneer study of the area. Cuen *et al*. (2013, 2016) redefined the geology of SJG and Buitrón-Sánchez *et al*. (2016) studied its ichnofossil content. This, altogether, has rendered a much clearer idea about the fossil content of these Lower Cambrian rocks and their paleoenvironmental and paleoecological meaning.

2.1. The Chihuarruita Hill in San José de Gracia

Oncolites studied in this paper come from Chihuarruita Hill, located in the vicinity of SJG, ~40 km East of Hermosillo (Figure 1). The fossil assemblages found at Chihuarruita Hill vary from Lower to Middle Cambrian, and represent well constituted marine communities of mature ecosystems. These communities include sponge-like animals (*Chancelloria* sp., *Diagoniella* sp.), acute-shelled molluscs (*Hyolithes* sp., *Haplophrentis* sp.), eocrinoids (*Gogia* sp.), brachiopods (*Acrothele* sp., *Dictyonina* sp.), trilobites (*Peronopsis* sp., *Ptychagnostus praecurrens*, *Bristolia* sp., *Olenellus* sp., *Oryctocephalites* sp., *Elrathina* sp., *Ogygopsis* sp., *Pentagnostus* sp.), and several types of ichnofossils (*Skolithos* isp., *Planolites* isp., *Arenicolites* isp., *Thalassinoides* isp., *Asterosoma* isp., *Palaeophycus* isp.; Buitrón-Sánchez *et al*., 2016). Their stratigraphic occurrence is indicated in Fig. 2 and some examples are shown in Figure S1. Oncolites are of course part of these assemblages, and coexisted for some time (> 1 Ma, judging by the thickness of the strata) with many shelled animals represented as fragments within the limestone matrix, and as nuclei of oncolites and within their laminae. Those shelled organisms were obviously reworked skeletal particles, commonly found in carbonate banks all throughout the Phanerozoic. The coexistence of oncolites with metazoans is unclear, given the absence of complete skeletons within the oncolitic limestone. Complete skeletons, however, are found in adjacent strata.

Four Cambrian rock units can be recognized at Chihuarruita Hill (figures. 1C, S2). From base to top they are the Proveedora, Buelna, Cerro Prieto, and El Gavilan formations (Cuen *et al*., 2016). The Proveedora Formation consists of cross-bedded quarzarenites with ichnofossils representative of the '*Skolithos* ichnofacies' (Buitrón-Sánchez *et al*., 2016). This formation was likely deposited in an intertidal to shallow subtidal, siliciclastic environment. Comparable lithology, ichnofacies and environmental interpretation has been proposed for the Proveedora Formation in the northern Caborca region (Rivera-Carranco, 1988a).

The second unit is the oncolite-bearing Buelna Formation that overlies the Proveedora Formation and grades up from mixed silicilastic-carbonate units to detrital limestone interbedded with shale. The oncolitic limestone is a ~1 m-thick, well indurated, calcitic limestone toward the mid section of the succession (figures 1, 2, S2). Toward the top of the oncolitic limestone a ~30 cm thick tempestite with abundant mud intraclasts crowns the last stage of the Buelna Formation and is in gradational contact with the overlying Cerro Prieto Formation in SJG. In the upper section there are abundant mollusks *Hyolithes sonora* and *Haplophrentis reesei*. These are associated with olenellid trilobites, identified as *Olenellus* sp. and *Bristolia bristolensis*, as well as *Gogia eocrinoids*, which indicate an age of 515–510 Ma (Levi-Setti, 1995; Cuen *et al*., 2016). The depositional environment of these strata is interpreted as shallow marine, with dominant low energy but with frequent high-energy storms and terrigenous input, perhaps in subtidal setting above the storm wave base (Cuen *et al*., 2016). We infer that the oncolites were accumulated within a carbonate bank flanked by a protected shallow area toward the shore.

The third unit, the Cerro Prieto Formation, consists of massive, dolomitized, oolitic limestone, with prominent cliffs and pronounced karstic features. Oolites are less than 1 mm in diameter (commonly 100 μm). Crystals of hematite and pyrite are common. The genesis and deposition of these oolites likely occurred in a high-energy, carbonate-supersaturated, shallow marine environment. High tide activity in a subtidal to intertidal environment can be envisioned for these facies. This Formation bears oncolites in the Caborca region (Cooper *et al*., 1952; Cuen *et al*., 2016) but not in SJG.

The fourth unit is the uppermost El Gavilán Formation. This top unit is composed dominantly of red shale interbedded with dark gray limestone, both with abundant trilobites, inarticulate and articulate brachiopods, sponge-like spicules, chancellorids, and hyolithids, among others (Figure 2, S1). Toward its base, brachiopods *Acrothele* sp. and *Linnarssonia* sp. are more common. The middle shale beds bear a wide variety of trilobites, including *Peronopsis bonnerensis*, *Pagetia resseri*, *Oryctocephalus* sp., *Oryctocephalites walcotti*, *Elrathina antiqua*, *Ogygopsys typicalis* and *Bathyuriscus* sp. (Cuen *et al*., 2016). Toward the top, sponge-like spicules of *Chancelloria eros* and *Diagoniella* sp. have been found (Cuen *et al*., 2013). The lithology and fossil composition suggest deposition within a middle to outer shelf. This formation bears oncolites in Nevada, USA (Cuen *et al*., 2016).

Overall, the sedimentary succession in SJG, depicts a change from silicilastic sandstone-dominated, to limestone-dominated, to shale-limestone lithologies. This could represent the deepening of the shelf, from coastal sands (Proveedora Quartzite), to a shallow carbonate ramp (Buelna and Cerro Prieto formations) and ending with episodes of deeper shelf environments (El Gavilan Formation)

where fine sediment (shale) was deposited, interrupting periodically carbonate deposition.

3. Methods

3.1. Sample collection

Oncolites were collected from a ~1 m-thick, oncolitic limestone unit (Figs. 2, S2) that is heavily recrystallized and less prone to erosion than the adjacent strata. Oncolite samples were chosen in situ after inspection with hand lenses to determine their degree of preservation, internal lamination, and non-laminated textures in order to have assorted representatives along a ~100 m stretch. Selected samples used for laboratory analyses were hammered out from the rock after being labeled with permanent markers (GPS location and spatial position within the stratum), and sealed in plastic bags.

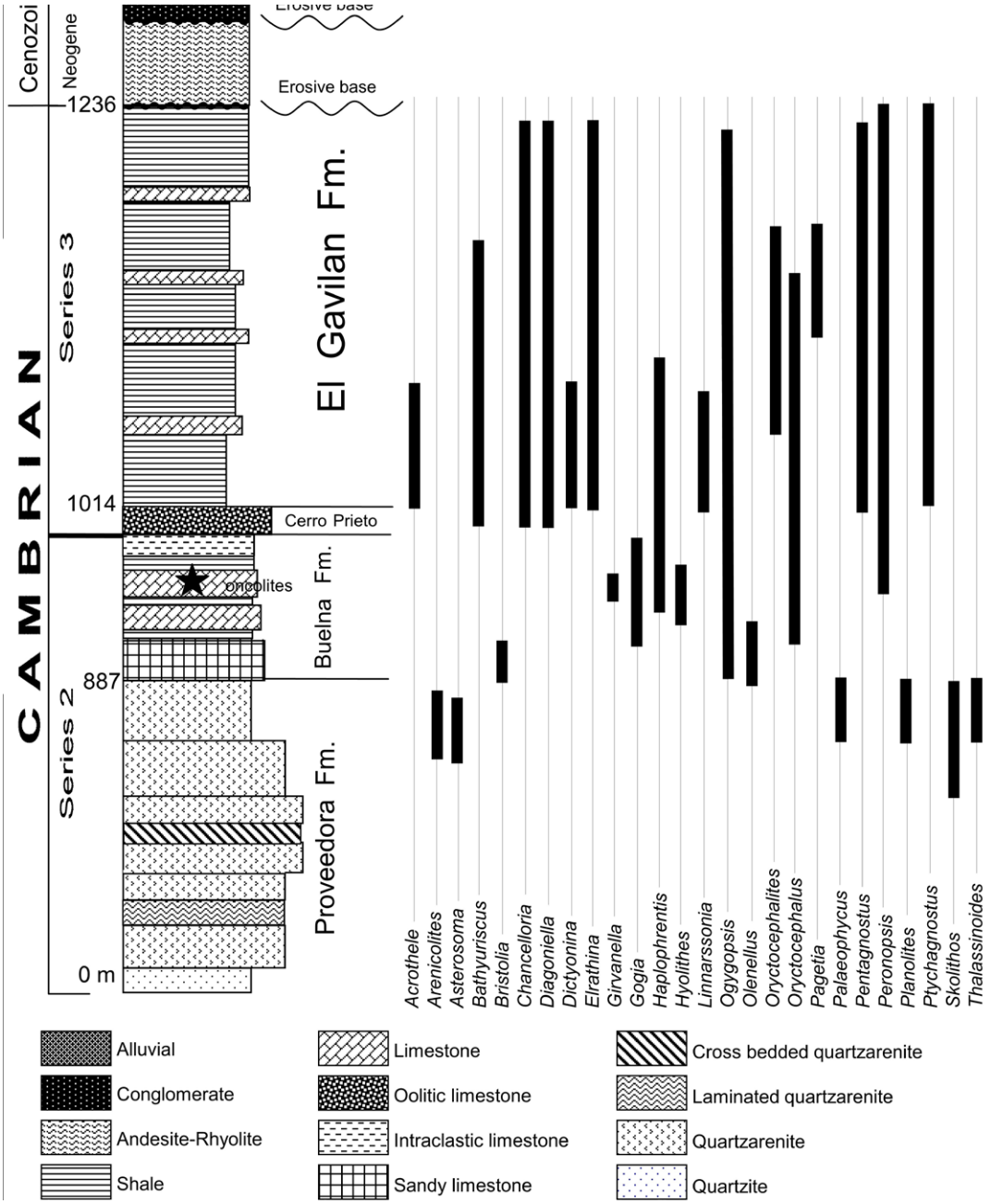

Figure 2. Stratigraphic succession of the Chihuarruita Hill indicating the approximate distribution of fossil fauna and ichnofossils. Some of this fauna is depicted in Fig. S1).

3.2. Size and density distribution

Measurements of oncolite diameters and areal density counts were quantified from 45 scaled images taken on the field along a ~100 m stretch of the stratum bearing oncolites, using a Canon D20 digital camera and the ImageJ free software v. 1.6 (https://imagej.nih.gov/ij). Areal density was calculated as the number of oncolites per unit area. Diameters were measured as the major axis of each oncolite in 2D at the rock surface (Figure S3).

3.3. Thin petrographic sections and polished surfaces

Polished surfaces and thin petrographic sections were used to observe diagenetic features (recrystallization, cementation, deformation, infillings, pressure marks, etc.), morphologies of aggregates, fossil content, and textures. These were made from 6 selected samples that were spread along the ~100 m stretch. They were observed and imaged in a Zeiss Axiozoom stereoscopic microscope, a Zeiss Axio Imager M2 brightfield microscope, and an Olympus BX51 petrographic microscope. The width of fossil filaments was measured from scaled images using the ImageJ software v. 1.6. Thin sections and fresh fractured samples were also observed with a Scanning Electron Microscope.

3.4. Raman analysis

Raman analyses were used to aid in the interpretation of possible organic remnants, such as graphitized contents in the oncolites and organic matter associated with iron compounds. Analyses were made from thin sections. A dispersive Nicolet-AlmegaXR (Thermo Electron Scientific Instruments LLC, Madison, WI USA) laser Raman setup was used, coupled with a BX51 Olympus microscope for focusing the beam repeatedly on a same target and averaging the peaks. The scattered light was collected in a 180-degree backscattering configuration. Raman spectra were accumulated over 25 s with a resolution of ~4 cm−1, the excitation source was 532 nm radiation from a Nd:YVO4 laser (frequency-doubled) and the laser power on the sample was 10 mW. The spectra were analyzed in Microsoft Excel v. 2003. The area under the peaks was calculated and the peaks were matched with a physical standard and standard curves from an owned CCADET-UNAM database.

3.5. X-Ray Diffraction and Fluorescence analyses

The bulk mineralogy and elemental composition of the samples was assessed with X-ray diffraction and X-ray fluorescence from powdered oncolites and bulk rock using a portable XRD-XRF Terra instrument (In Xitu Inc.; Bish *et al*., 2007), with a Cobalt X-ray tube at 40 Kv and a fixed 5 to 50-degree 2Θ and a resolution of 0.3 degree 2Θ. Detected X-rays were integrated by default into a histogram of number of photons and photon energies that produced a XRF pattern of the sample. Data analysis was made using the JADE software v 7.0 (MDI, Pleasanton, CA) and the ICDD (www.icdd.com) and AMCSD (http://www.geo.arizona.edu/xtal-cgi/test) library data.

3.6. Scanning electron microscopy with elemental analyses

Thin sections, fresh fractures, and HCl-etched fragments of oncolites were observed, uncoated, in a variable-pressure Zeiss EVO10-MA Scanning Electron Microscope, equipped with a Bruker Flash X electron dispersive spectrometer (EDX), to image the samples at the nano-scale and to observe fine microscopic details, as well as the elemental composition depicted by X-ray elemental mapping.

4. Results

Abundant (201–996 oncolites/m^2; average = 465; Table S1) grey to black oncolites, semispherical and concentrically-laminated, were enclosed in a hematized matrix of skeletal grains, oolites, and, locally dolomitized, calcite (Figure S3). Their diameter ranged from 2 to 44 mm (n = 2226; Table S1), being more frequent from 8 to 15 mm (Fig. S3). These measurements may be biased, as the exposed cross sections from which measurements were made may not represent the central axis of symmetry of the oncolites, but rather oblique cuts. Regardless, it is a numerical value useful for comparisons against other Cambrian oncolites.

Most of the oncolites were nucleated on mollusc shells (*Hyollites* sp.), which appeared filled with micrite and thin and assorted, broken skeletal grains (figures 3, 4). The oncolites and the matrix (60–80% skeletal grains) were pervasively hematized (figures 3, 4), although some portions were enriched in silica (figures S4A, S5). Skeletal grains were mostly calcitic, but displayed heterogeneous composition (figures S4–S9). Carbonate recrystallization and cementation often displayed drusy habits (Figure 3 D), which indicate a synsedimentary or early diagenetic process of cavity filling. A small percentage (< 5%) of terrigenous particles (floating quartz grains and Fe-rich, clay-sized aggregates; figures 3 B, D, F) were also observed. Hematization may have been selective, as some buried contents display heterogeneous hematization (figures 3 E, F). This pattern suggests that some hematization processes were syndepositional or early diagenetic. Some oncolites displayed corroded surfaces (karstic textures) and small pits, which were then covered by a new laminae (figures 4 C–D, 5). These could have been produced by erosion or bioerosion (grazing, cyanobacterial boring, etc.). Some oncolites displayed relatively large burrows perpendicular to the concentric lamination, sometimes distorting it (Figure 4 C). The burrows were usually filled with slightly finer sediment than the surrounding matrix (figures 4 C–D, 5). Bioerosion

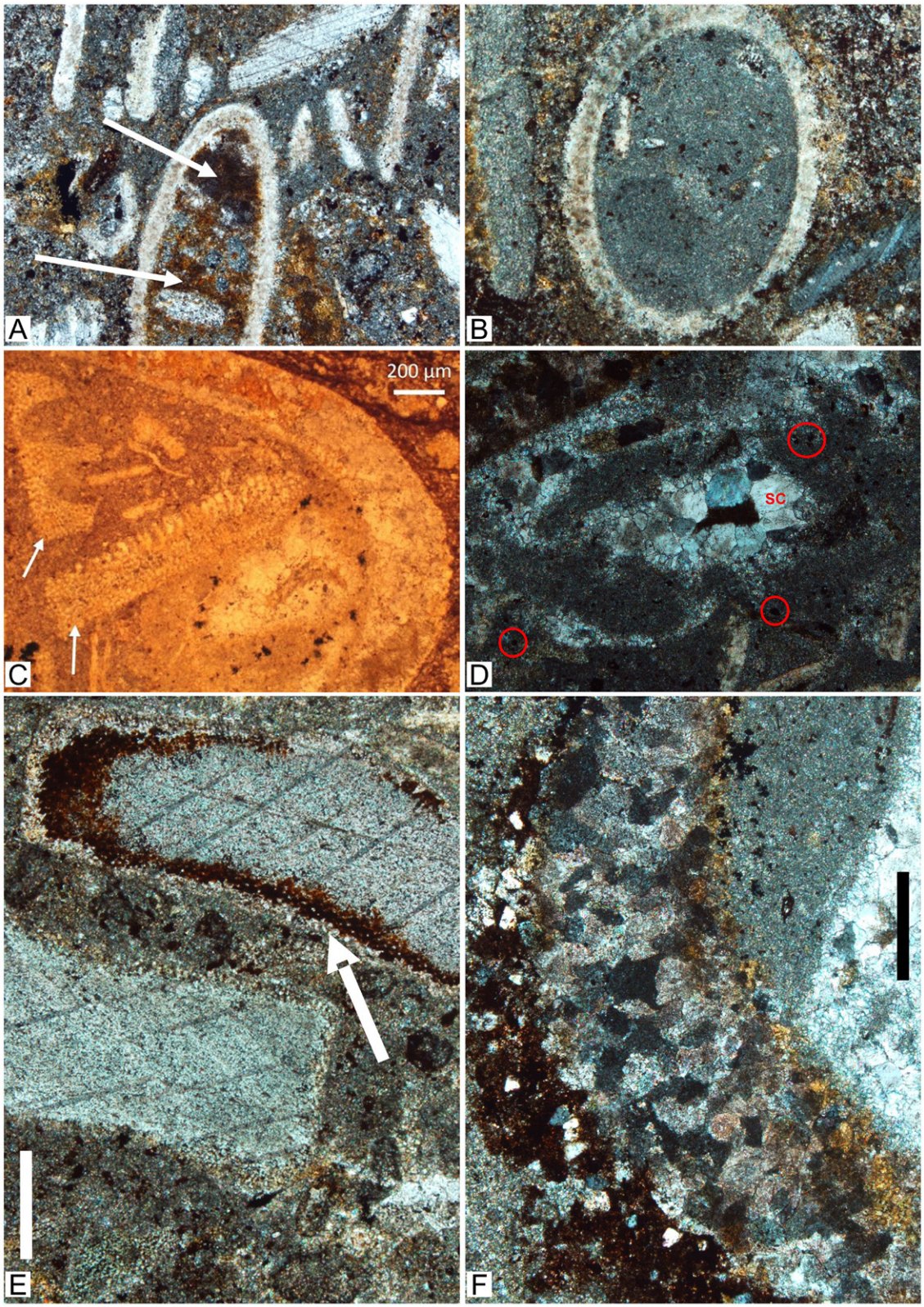

Figure 3. Cambrian oncolites from San José de Gracia at the mm to cm scale. A. Oncolites embedded in a hematized limestone-dolostone. The 'packstone' matrix is dominated by eocrinoid, trilobite, mollusc, and brachiopod fragments. M = mollusc nucleus; O = Oncolite. Mx = matrix. Scale = 10 mm. B. Close up of an oncolite to show its concentric laminations (L), the previously-filled mollusc nucleus (N), the skeletal packstone matrix (M), and the pervasive hematization all throughout. Note corroded surfaces and interiors (arrows), and the cross-cut lamination (curved lines). Scale bar = 5 mm. C. Dominant skeletal grains. Large fragment of an eocrinoid (e), along with smaller brachiopod, and trilobite (t) fragments. The oncolite surface displays accreted sediment wrapped by an outer lamina. Distorted lamination can be produced by grazing and burrowing of other organisms. Scale bar = 5 mm. D. Naked (m) and encrusted (o) mollusc shells, along with fragments of eocrinoids (e) and trilobites (t). Scale bar = 5 mm.

at different metric scales is plausible, and was likely made by different biological groups (*e.g*. bacteria, fungi, protozoa, and animals), which were present at the moment, according to the fossil record of the Chihuaurrita Hill.

Concentric, usually discontinuous, sub-millimetric, micritic laminae outlining the oncolites could be seen at macro and microscopic scales (figures 4–6). Laminae could be thin (3–20 µm), medium (20–200 µm), or thick (> 200 µm), smooth or contorted, and sometimes appeared cut by other laminae, indicating erosion events (figures 4 B, 6 A–D). In many cases, biofilm-like textures were present, usually lined up by several episodes of laminar development

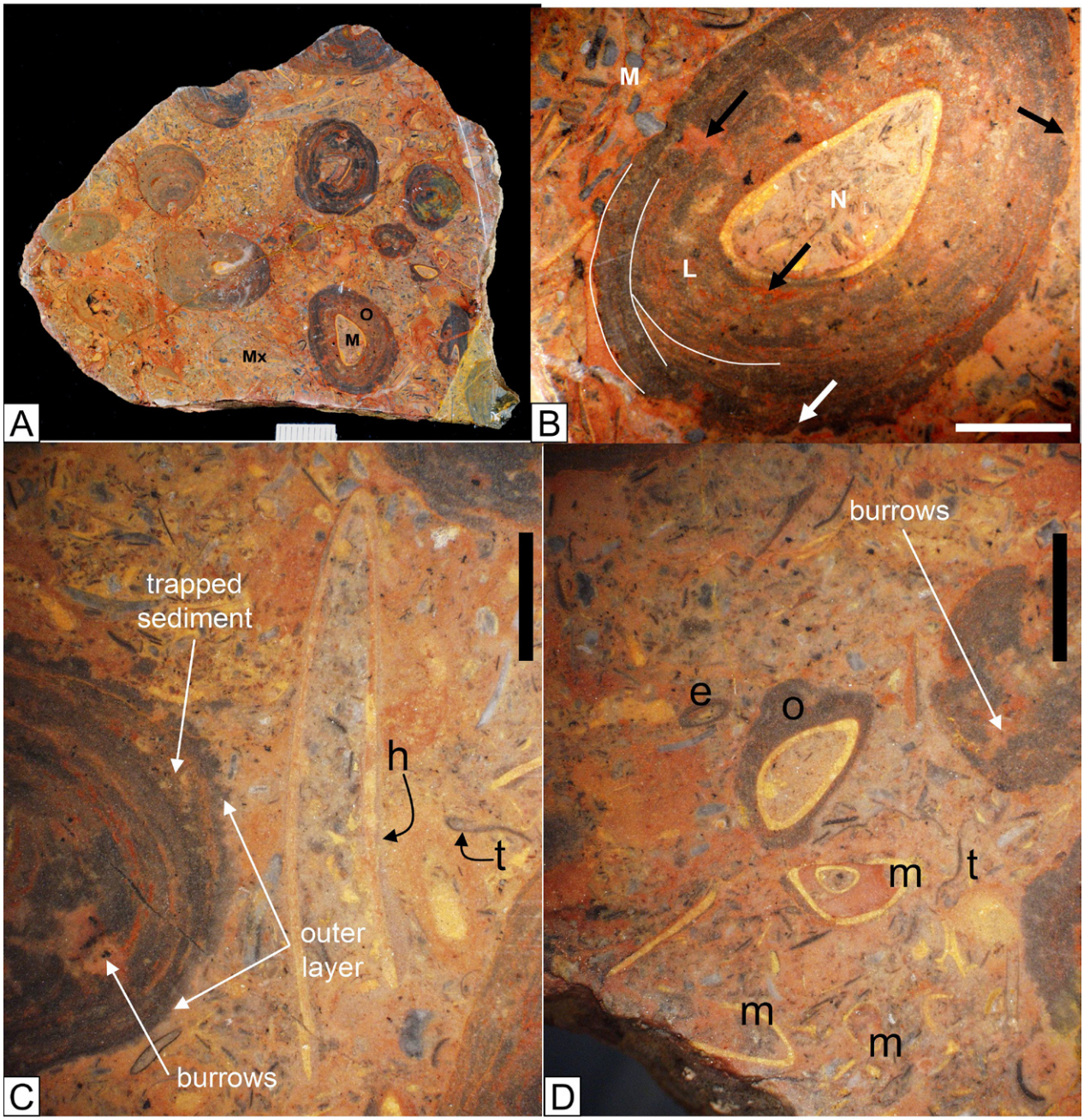

Figure 4. Distinct filling of skeletal grains and hematization. A. note the selective hematization (arrows) inside the largest eocrinoid shell, compared to the less hematized exterior matrix. B. Finer, micritic, and less hematized sediment inside the elyptical eocrinoid shell, compared to the coarser and heavily hematized exterior matrix with terrigenous particles. C. Eocrinoid fragments (arrows) inside the nucleus of an oncolite. D. Pore spaces being filled with sparry calcite with drusy habit (SC). Note micritic matrix with scattered terrigenous particles (circles). E. close up to eocrinoid fragments showing their characteristic twinning lamellae. Note degradation and hematization toward the edges of the fragments (arrow). F. close up to a brachiopod shell, showing exterior and interior coating of walls (dark). Terrigenous particles can be seen otside the shell as part of those coatings. Scales in A and B = 5 mm. Scales in C and D = 250 µm.

(Figure 6 B–D). Biofilm fragments and accumulations of dark kerogenous material were also present in the best preserved samples (Figure 6 E–F). Such organic materials could be seen coating grains, forming clumps and ripped biofilms, and were constituted by different densities, porosities, and textures, either in biofilm-biofilm contact or in biofilm-sediment contacts (figures 6–8). In some cases, fenestral porosity infilled with sparry calcite (figures 7 E–F, 8 C–D) were similar to biogenic, gas-like accumulations (see figures 3–4 in Wilmeth *et al*., 2015).

Girvanella-like filaments were pervasive in most samples (figures 9–10), along with other tubular filamentous structures (Figure 11). Some of them had sinuous morphology and irregular width (Figure 9 D), which might be compatible with fungal hyphae. These did not display diagnostic features, such as sporangia or other reproductive structures, perhaps because the entire length was not observed in full, but in fragments only. The *Girvanella*-like filaments were 2.7 to 13 µm in width and > 100 µm in length, with an average width of 5.8 µm and a median of 4.6 µm (n = 50). No filament branching was observed, although the intrincate nature of the contorted filaments holds doubt on this fact. In cases where filaments could be 'followed' in length, a fairly constant diameter was observed. Some filaments appeared to be septate (Figure 9 D–H), but lack of consistency in supposedly 'septal' walls may imply crystal growth within the filament cavity rather than true original septa. This needs further studies to be confirmed.

Secondary and backscatter SEM images of different portions of oncolites (figures12–14) revealed the presence of tubular, subspherical, and amorphous, biogenic-looking structures that were partially preserved. Most of them were siliceous in composition (figures S4–S9) and often enriched in iron. Other Fe-rich, isolated structures were also found within the oncolitic lamination (figures S4 A, C, S5 B, S6 A-B, S8 B–C). In cases where Al-enriched areas were more prominent, Fe was scarcer or absent. The Carbon signal from EDX seemed to be associated largely with Ca, indicating its presence in the form of $CaCO_3$ of the shells, the rock matrix, and the oncolites. However, it sometimes appeared concentrated in structures of uncertain, but likely biogenic origin (Figure S5 D). Raman spectra with clear G and D bands obtained from the samples were consistent with the presence of kerogenous material within the structure of the oncolites (figures S10–S11), and argues for some original organic material to be present in the rocks, as is the case in other fossil examples of older and younger ages (Schopf and Kudryavtsev, 2009; Beraldi-Campesi *et al*., 2015). XRD analysis detected 80% calcite in bulk rock matrix and oncolites separately, with minor (< 20%) quartz and muscovite (Figure S12). XRF analyses (Figure S12) showed the presence of Ca, Mn, Fe, and Co, from which Ca, Fe, and Mn were measured also with EDX (figures S7 B, S8 A, S9 A). Mg was also detected with EDX (figures S7 A, S8 A) but not with XRF. Further studies may require analysis with a different methodology (*e.g*. solvent extraction, mass

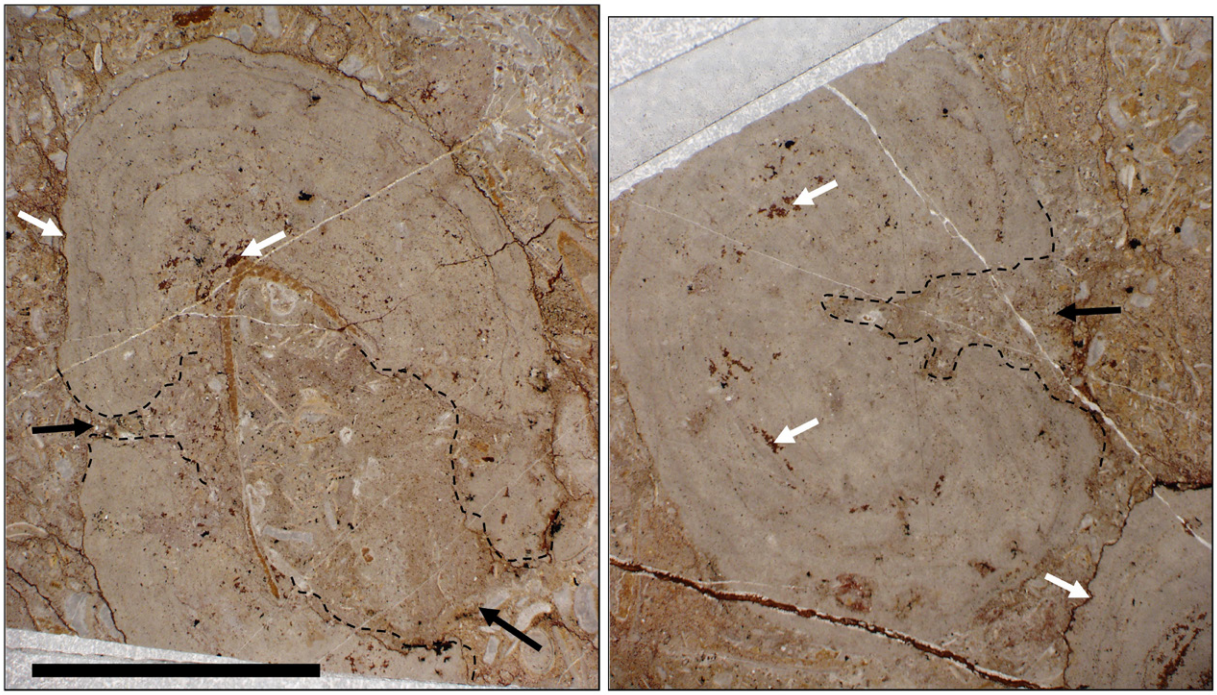

Figure 5. Pits and burrows in oncolites. A nucleated (left) and non-nucleated (right) oncolite displaying burrows, inner pits, and corroded surfaces. Dashed lines show the burrows and black arrows show their entrances. Eroded (karstic) or bored surfaces and pits are shown with white arrows. Scale bar = 1 cm for both images.

spectrometry) to better analyze organic compounds and metals.

5. Discussion

5.1. Environmental significance of oncolites

The presence of oncolites in the sedimentary Cambrian of Mexico demonstrates the wide geographical distribution that such microbialites attained in the past, and therefore, the significant importance of microbes in sedimentary and biogeochemical processes throughout time. Fossil oncolites are known from the Precambrian (3500 Ma) to the Recent, in a variety of environments (Henderson, 1975; Dunlop *et al*., 1978; Lowe, 1983; Knoll *et al*., 1989; Winsborough *et al*., 1994). The studied oncolites mark an important episode of microbial-sediment development in this part of southern Laurentia in the Lower Cambrian.

Oncolites may constitute good indicators of microbially-induced mineral precipitation rates in relation to their size in non-saturated solutions. Thus, the presence of relatively

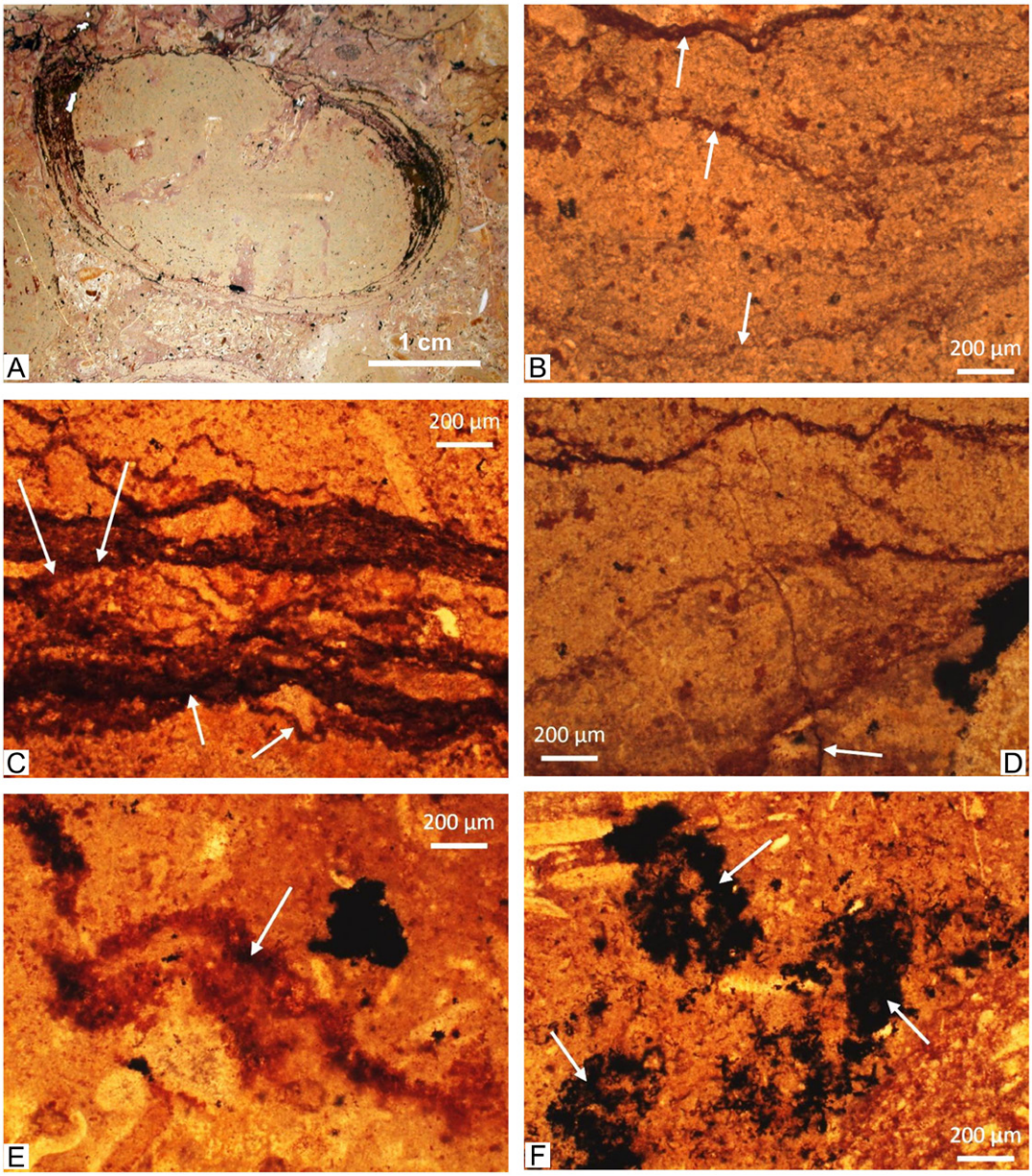

Figure 6. Oncolite lamination and biofilms. A. Oncolite with a muddy core (no shell nucletion) and well developed biofilm lamination toward the surface. B. Oncolite lamination showing biofilms (arrows) spaced by relatively long intervals of sediment accumulation. C. Biofilm lamination showing relatively short intervals of sediment accumulation. Example of erosive surfaces of biofilms are indicated with arrows. Each lamina indicates an event of biofilm formation. D. Fractures crossing oncolite lamination. Fluids can migrate easier through fractures and transport organics and metals. E. Ripped piece of biofilm of ferruginous organic matter. F. Graphitized and ferruginous organic matter. Note some grains coated with it.

large, marine carbonate oncolites would imply high rates of mineral precipitation, likely associated with microbial productivity, in particular high rates of photosynthetic CO_2 sequestration (Kah and Riding, 2007), which is important for the CO_2–CO_3 balance in the oceans and essential in the global carbon cycle. It also may imply high rates of microbial sulfate reduction, as it appears to be one of the main process of lithification in modern, marine, carbonate stromatolites (Dupraz and Vischer, 2005). These features are highlighted in the studied oncolites, which are relatively large and abundant, implying an important sink for carbon by this time.

Regarding the local environmental conditions, the great abundance of reworked and fragmented skeletal grains in the matrix and inside the studied oncolites, suggests episodes of high-energy and reworking capable of grinding shells. This high-energy is consistent with the energy required to overturn the oncolites and promote their concentrically, laminated growth. Smaller, reworked skeletal grains filling larger shells (Figure 3A), suggest that there were

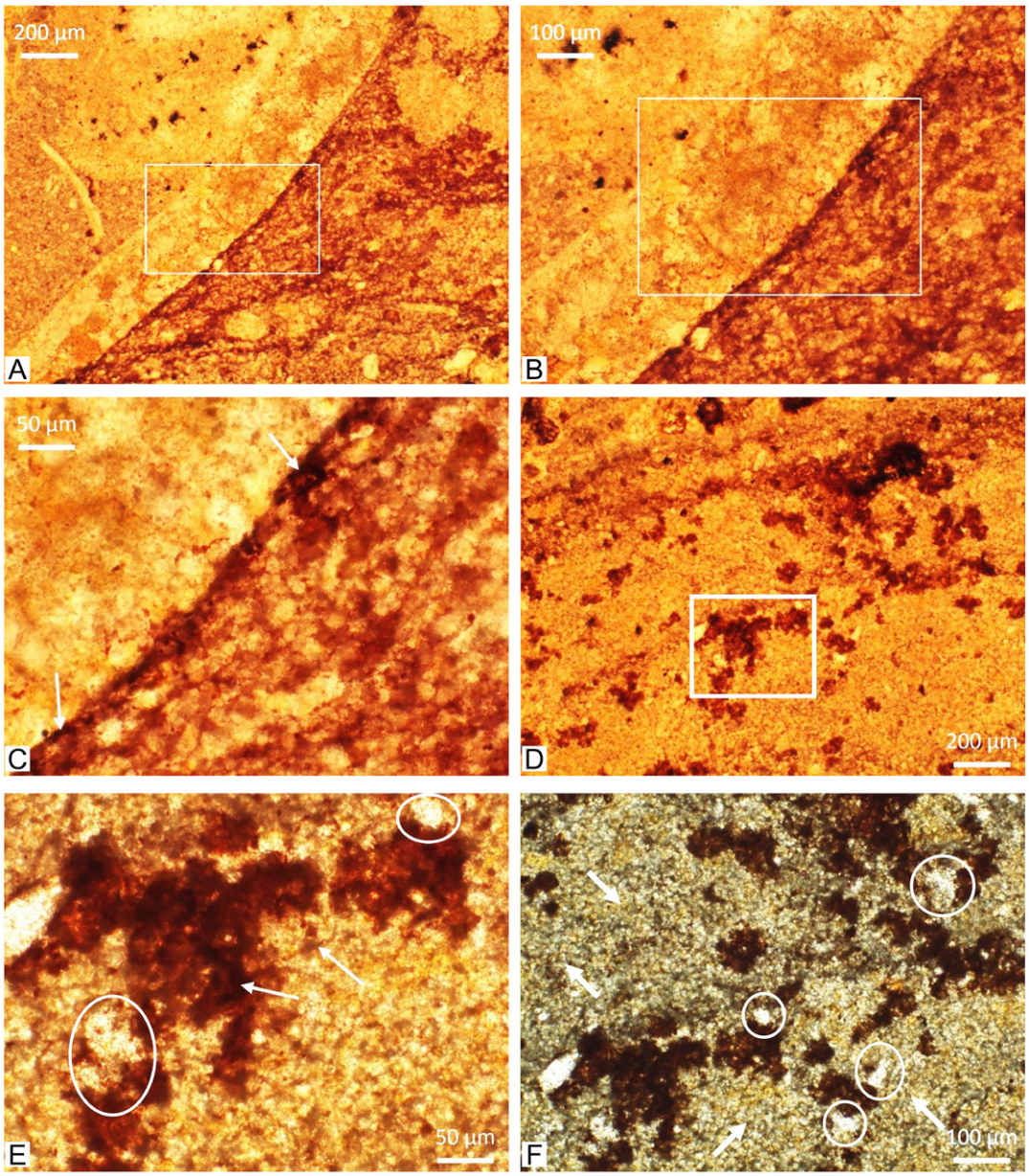

Figure 7. Oncolite biofilms and their interaction with *Girvanella*-like filaments. A. Well preserved oncolite nuclear boundary. B. Close up of box in A showing the and organic-rich layer. C. Close up of box in B. Coated grains (arrows) in the organic matrix can be seen in contact with the mollusc shell. D. Clumped organic material distributed along the oncolite laminae. E. Close up of box in D showing filament-like structures associated with organic clumps. Fenestral porosity filled with sparry calcite (circles) indicate gas-like voids. F. Same clumps shown in D and E, in polarized light. Note the abundance of *Girvanella*-like filaments (arrows) occupying spaces between clumps. Circles indicate fenestral porosity formed through gas accumulation.

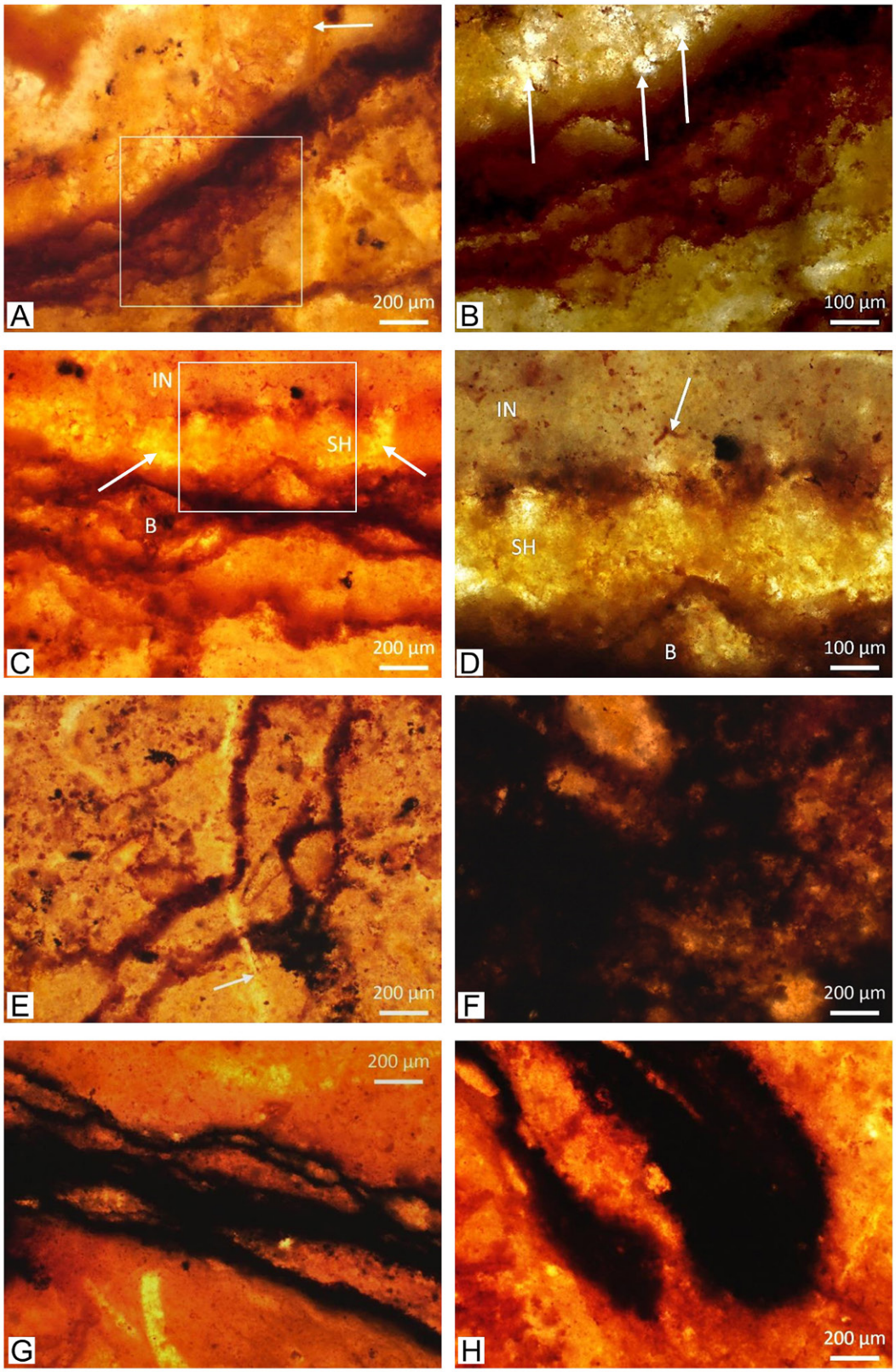

Figure 8. Oncolite biofilms. A. Biofilm at the boundary of a lamina, showing abundant microbe-like structures (arrow). B. Close up of box in A showing dark laminations developed by biofilms and the mineral grains embedded in them. Arrows show fenestral porosity, likely derived from metabolic gas production. C. Laminated biofilms (B) covering a shell fragment (SH) and the sedimentary fill of the interior (IN) of the nucleus. Arrows point to gas-generated fenestral porosity filled with sparry calcite. D. Close up of the filament shown in C. Mucilaginous cover and cells are overdrawn with a dashed line. E. Peculiar lamination crossed by a fracture (arrow). F. Sometimes organics are concentrated. G. Well stained ripped laminated biofilm. H. Rounded end of biofilm shown in C. Thread-like structures may be seen departing from the main structure by the bottom end.

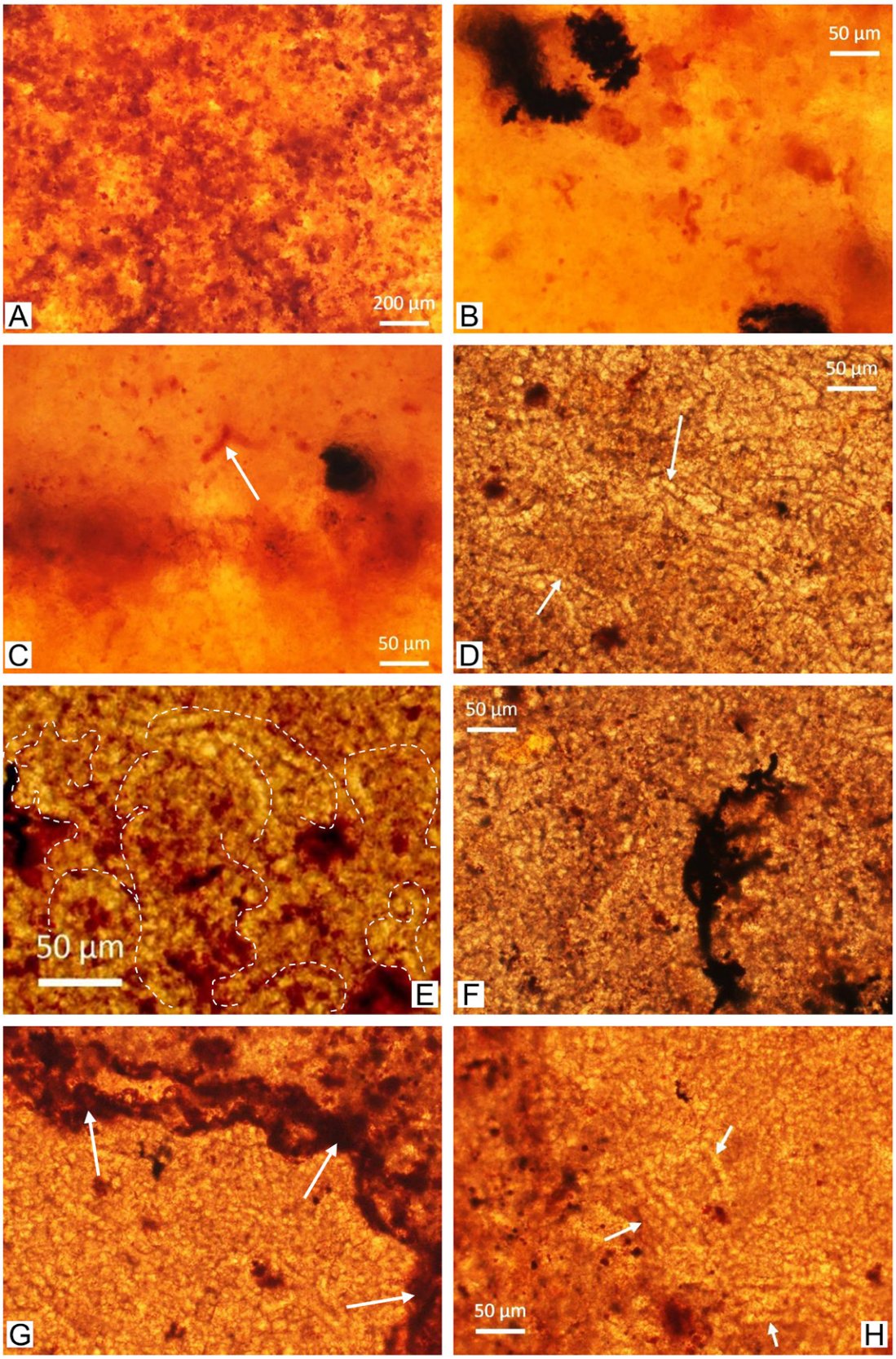

Figure 9. Filamentous structures. A. Filament-like structures that form part of an oncolite lamina. B. Close up of isolated filament-like structures shown in A. C. Isolated and contorted filament-like structures (arrow). D. *Girvanella*-like filaments displaying an overall NW-SE alignment. E. Close up of the lower left area in D, displaying *Girvanella*-like filaments with marked curvature (dashed lines). F. Dark fungal-like structure surrounded by *Girvanella*-like filaments. G. *Girvanella*-like filaments delimited by a biofilm (arrows). H. *Girvanella*-like filaments showing septation (arrows).

previous episodes of sedimentation, early diagenesis, and reworking, before they were deposited in the basin. Riding (1975) has stated that *Girvanella* (likely cyanobacteria) can develop in shallow waters (< 30 m), with depth ranges that may vary from a few meters to several hundred meters or more. The amount and density of oncolites in SJG can be better explained in a high energy environment with wave oscillation for their overturning. This would require a shallower environment less than 30 m deep. Even in clear, oligotrophic waters, where photosynthesis could have operated in deeper waters, no sufficient energy would have been available for the rolling needed to form oncolites.

Remnants of semi-preserved organic matter (figures. S6 C–F, 8, S10) indicate that a rapid process of entombment occurred, perhaps in oxygen-deficient conditions within the sediment, which prevented its oxidation (Bauld, 1981; Zonneveld *et al*., 2010). Cavities with patterns of microbe-sediment-gas interactions preserved within the oncolitic lamination (Figure 8 B–D), could be correlated with deformation of the original biofilm by gas entrapment (Wilmeth *et al*., 2015). This is plausible given the existence of conspicuous biofilms and colonial filaments (figures 6–11) that likely produced gasses within the oncolite lamination while this was developing. We infer that abundant microbial communities, including cyanobacteria, were responsible for the development of the SJG oncolites, that they developed in a carbonate, shallow bank with episodes of storms and high-energy currents, and that fine sediment accumulated rapidly and entombed a large proportion of specimens, where anoxic conditions and early diagenesis occurred.

SEM analyses support the idea that some microbial remains were fossilized and are still present in the samples. Despite the degree of obliteration due to diagenetic processes (including replacement and recrystallization), carbon peaks in EDS of some biogenic-looking structures and clear G and D bands in Raman spectra, indicate the presence of organic matter localized in specific regions of the samples. Some of these organic remains appear to have been silicified and enriched in Fe. Complexation of metals by sorption on microbial EPS is common in most environments, and it keeps those metals bound or chelated (Sander and Koschinsky, 2011) and even dissolved for several days (Theis and Singer, 1974). Combined processes of metal sequestration and early diagenesis may be reflected in specimens where oncolite lamination was highly enriched in Fe (Figure S8 C). The selective hematization in some cases (Figure 3 E–F) is also indicative of this process, by the chemical alteration of isolated fragments that experienced diagenesis before being transported and redeposited where the oncolites were forming. Infilling of pores with sparry calcite in drusy habit suggests episodic transitions from saturated conditions below the water table, to unsaturated conditions within the vadose zone, where cavities could have been infilled with calcite. It is possible that sea level fluctuations (tides) or prolonged seasons of subaerial exposure in the carbonate bank influenced the early diagenetic history of the oncolitic deposit.

The SJG oncolites also display features that may be of ecological relevance. Corroded and perforated fabrics (pits) observed in our oncolites (figures 4–5) may be indicative of microbial boring, which is common in these environments (*e.g*. Garcia-Pichel *et al*., 2010), and also indicative of feeding processes of grazers on soft or semi-lithified surfaces. Metazoans (especially eocrinoids, mollusks and trilobites) could have fed on microbial biofilms and mats. The absence of stromatolites in the SJG but large amounts of oncolites may have been influenced by grazing. Sesile microbialites could have been easily targeted by metazoans contrary to the mobile oncolites. The different size of the cavities may reflect grazing intensity and body size of grazers and borers. In addition to bioerosion, karstic dissolution (whenever exposed to the atmosphere) and abrasion caused by rolling of the oncolites are likely to have occurred as well. These small-scale interactions require further studies.

5.2. Interpretation of *Girvanella*

The genus *Girvanella* was first described by Alleyne Nicholson and Robert Etheridge in 1878 from Upper Ordovician exposures near Girvan, on the Ayrshire coast, UK (Nicholson and Etheridge, 1878). The description reads: “Microscopic tubuli with arenaceous or calcareous (?) walls, flexuous or contorted, circular in section, forming loosely compacted masses. The tubes apparently simple cylinders, without perforation in their sides, and destitute of internal partitions or other structures of similar kind” (Nicholson and Etheridge, 1878). Microbes influence the development of oncolites, either by promoting mineral nucleation and precipitation, or by affecting the porosity, lamination, and other internal fabrics, as well as the three-dimensional development of the structure. Although many microbes can be present in oncolite-biofilm communities, cyanobacteria are the typical type found in association with this type of structures in shallow marine and freshwater environments (Winsborough *et al*., 1994; Wade and Garcia-Pichel, 2003; Alshuaibi *et al*., 2012). It is probable that cyanobacteria dominated these environments and were dominant drivers of oncolite-associated biofilms (Riding, 1975, 1977). The presence of *Girvanella*-looking filaments in these Sonoran oncolites supports this hypothesis but makes no reference to any specific taxa at the moment. Proof of their biological origin is the abundance of filamentous structures that, given their curvature and spatial arrangement, fit the minimum criteria for biogenicity, along with their contextual provenance, indigenousness, and syngenicity (Buick, 1990; Schopf, 1993). We assume that cyanobacteria were present in the environment where SJG oncolites formed, that they had a crucial role in oncolite formation, and that they were responsible for much of the primary productivity at the time.

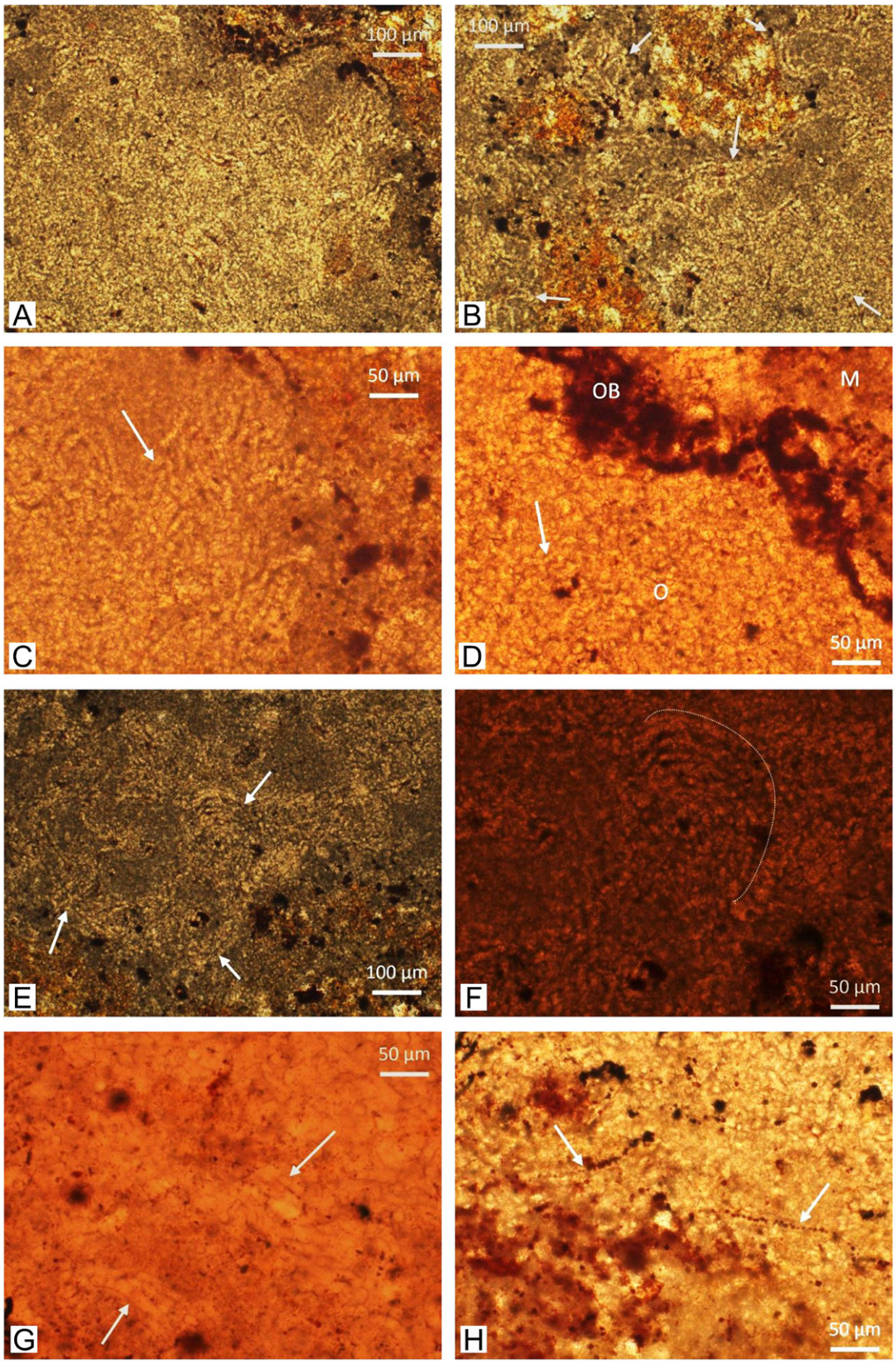

Figure 10. *Girvanella*-like filaments. A. *Girvanella*-like filaments filling a space inside an oncolite. B. *Girvanella*-like filaments (arrows) near hematized areas (reddish). C. Close up of the *Girvanella*-like filaments shown in A and B. D. Septated *Girvanella* filaments (O) (arrow) next to the organic-rich biofilm (OB), separating them from the matrix (M). E. *Girvanella*-like filaments forming a coil in polarized light. F. Close up of a *Girvanella* coil in transmitted light. G. *Girvanella*-like filaments forming coils in groups. H. *Girvanella*-like filaments sharing space with larger, and morphologically different types of filaments.

Stratigraphically, *Girvanella* is found in the Neoproterozoic and throughout the Paleozoic and Mesozoic (Riding, 2006). It tended to grow in shallow marine and coastal environments, where it was pervasive in microbialite-building communities. Their physiology and metabolic consequences for the environment (biogeochemistry), along with their capacity to interact with minerals, must have been significant as geobiological agents. The *Girvanella*-oncolite association seems to be common in the Lower Cambrian of Sonora and other parts of the world.

The *Girvanella*-like filaments found in SJG may differ from the original description by the apparent presence of septa in most of the filaments (Figure 9 D–H), but are similar in size and spatial arrangement. It should be noted that septate-looking and branching *Girvanella* (which by definition should be non-septated and non-branched) have been reported from the Ordovician of Scotland (Wood, 1957). The physiological nature of these microfossils is uncertain, but a cyanobacterial origin cannot be discarded (Wood, 1957; Riding, 1977; Laval *et al*., 2000; Planavsky *et al*., 2009). Filaments forming coils (figures 9 E, 10 E–F) may portray behavioral traits also observed in cyanobacteria (Shepard and Sumner, 2010; Sim *et al*., 2012). Some biomorphs (filaments, blobs, subspherical features) within

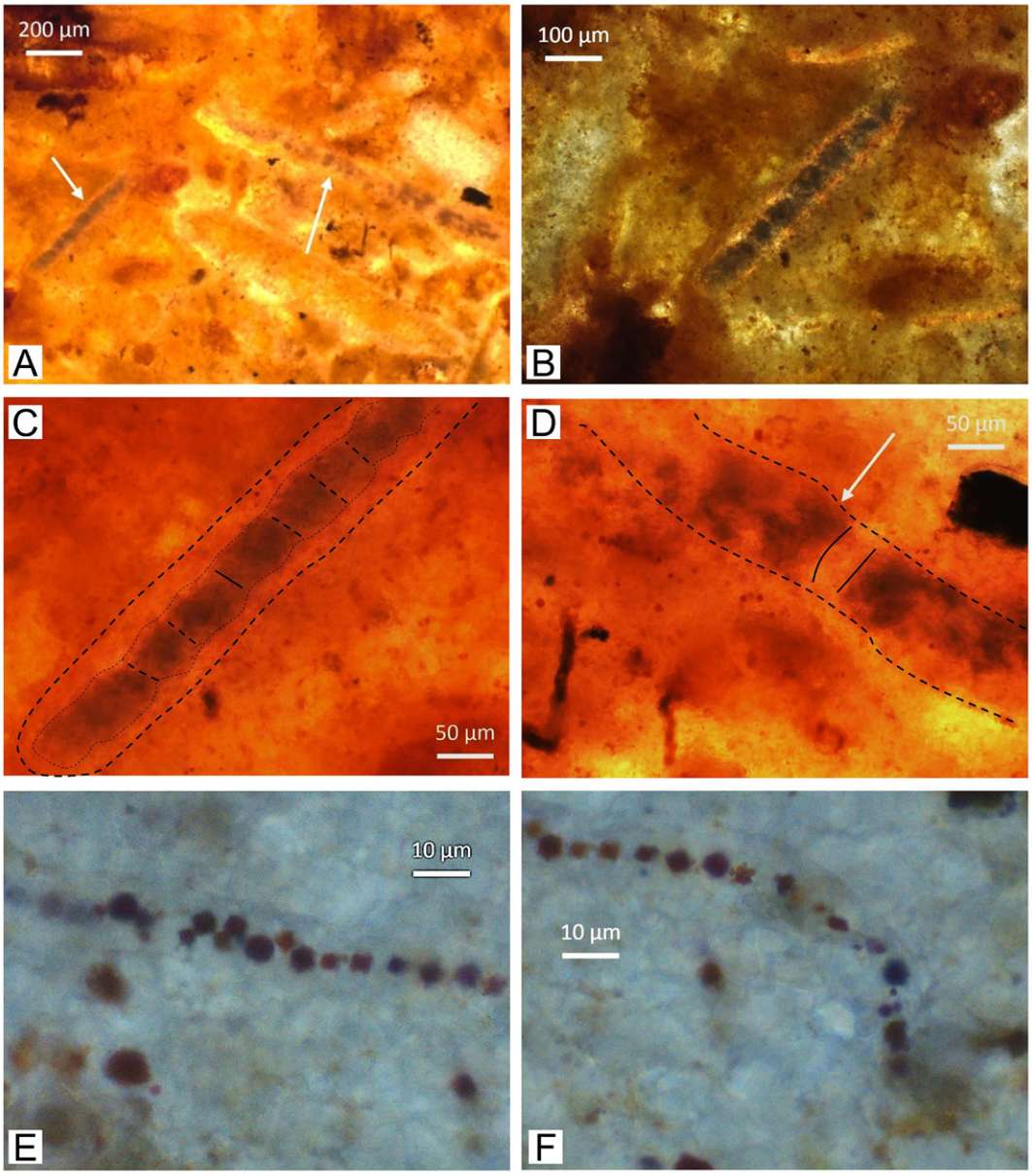

Figure 11. Other types of filaments. A. Filamentous structures (arrows) in the matrix between oncolites. B. Filamentous structure with septation and mucilage-like cover surrounding the trichome-like arrangement. C. Close up of the filament shown in B. Mucilaginous cover and cells are overdrawn with a dashed line. D. Close up of filament (dashed lines) shown in A. Cell-like bodies (arrow) seem to be separated by a septum (solid lines). Fungi-like organisms are also present (bottom left quadrant). E. Close up of filaments shown in B. F. Close up of a filament displaying flexibility.

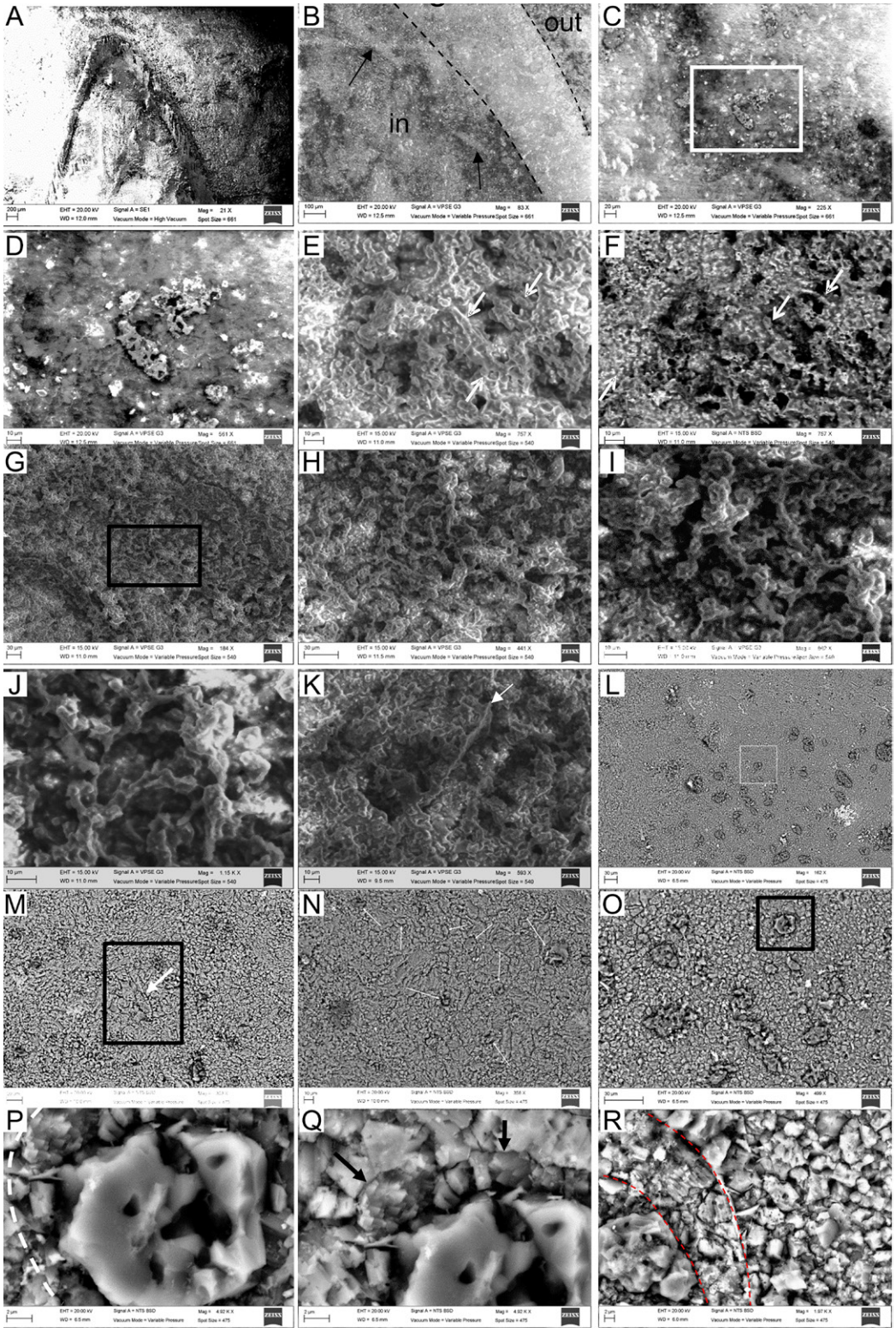

Figure 12. SEM photographs of the oncolitic structure. A. Fresh fracture of an oncolite displaying its nuclear mollusc shell, the inner filling with skeletal fragments, and the outer oncolite massive texture. B. Brachiopod shell (dashed lines) between inner filling with skeletal grains (arrows) and outer oncolite body. C. Oncolite matrix and part of the internal lamination (dark), displaying cross sections of filament-like structures. White box shown in D. D. Detail of the acid-etched cross section of a filament-like stucture. EDS of a similar structure is in Fig S4A. E–F. Oncolite matrix with clumps of calcite and occasional filamentous structures (downward arrows), sometimes with buddying-like structures (upward arrows). F = secondary electrons. G = backscatter electrons. G–H–I–J. Different magnifications on biogenic-looking features. K. Calcitic matrix of a fractured oncolite (arrow). L–M–N–O–P–Q. Different magnifications of a portion inside the oncolite matrix. Silicified cross sections of filament-like structures appear in the surrounding. Note the cell wall-like structure in P and Q (dashed line and arrows). See figure S4 for EDS analysis of the filament-like structures. R. Crystal size, not composition, makes cell wall-like structures visible (dashed lines).

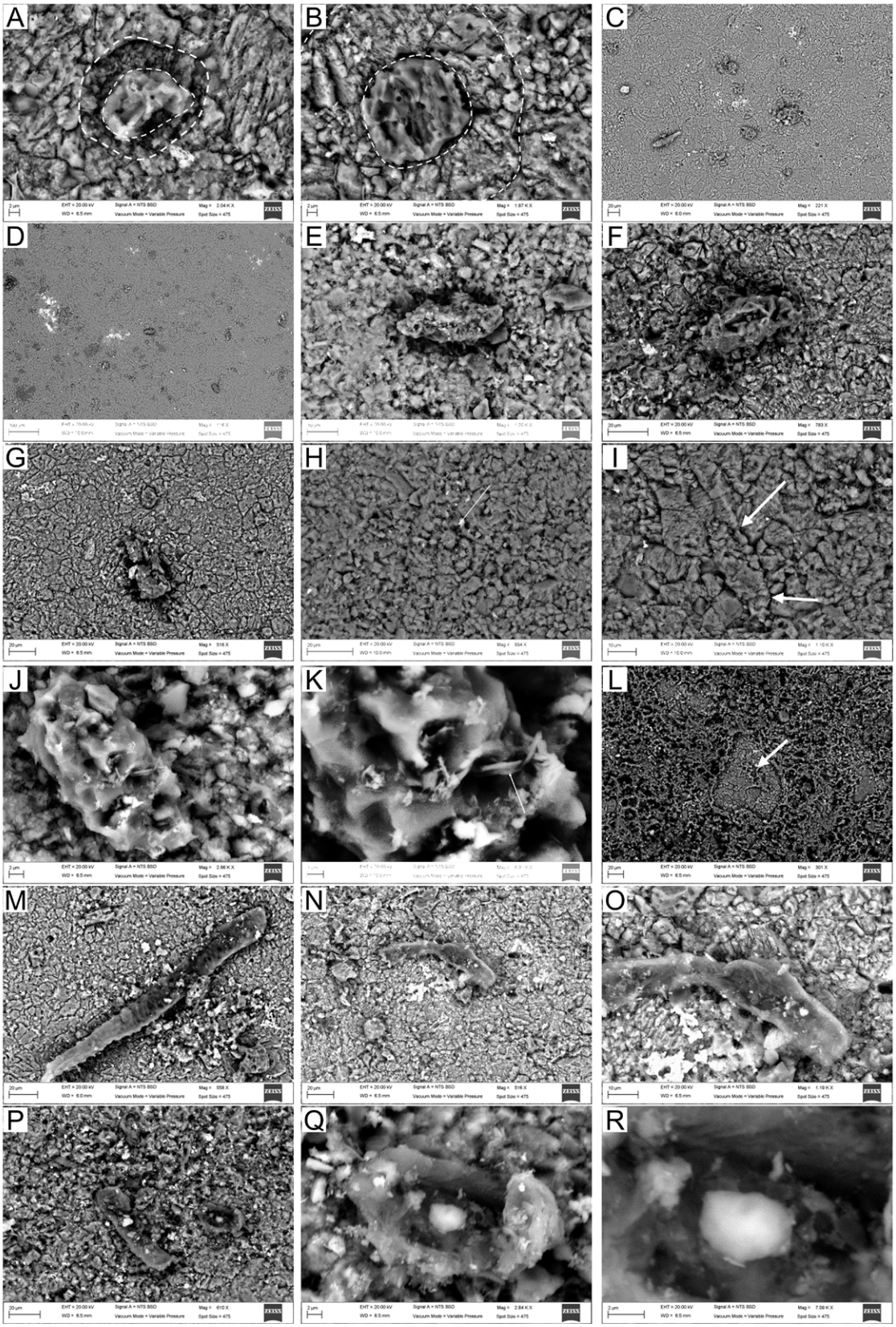

Figure 13. SEM photographs of the inner oncolite structure. A–B. Cell wall-like structures around filament-like structures in cross section. C–D. Limestone matrix with filament-like structures in cross section. E–F–G. Close up of filament-like structures in cross section in D. Cell wall-like structures are absent. H–I. *Girvanella*-like filament (arrows). J–K. Siliceous core of a filament-like structure showing porosity and clay minerals. L. Calcified and carbonaceous body (arrow) surrounded by silicified structures in a honeycomb-like texture. See Fig. S7 for EDS elemental analysis. M–N–O–P. Close up of carbonaceous, tube-like structures. Q–R. Cross section of a tube-like structure with a siliceous core.

Sonoran oncolites could be compared with reminiscences of calcifying biofilms seen in ancient (Riding, 2006) and modern marine microbialites (Planavsky *et al*., 2009). If cyanobacteria inhabited these biofilms, they must have been responsible of important biogeochemical cycling and ecological and geobiological functioning.

5.3. Stratigraphic significance

The Cambrian outcrops of the Chihuarruita Hill site bear important index fossils for biostratigraphy and age correlation (Figure 2). For instance, the eocrinoid *Gogia granulosa* has been reported also from northern Utah and south-eastern Idaho (Robison, 1965; Sprinkle, 1973; Nardin *et al*., 2009) and indicates an Early to Middle Cambrian time span. Trilobites are abundant and diverse in Sonora and useful for global age correlations. Numerous genera of agnostoid arthropods (*Peronopsis* and *Pagetia*) have been identified in Sonora, India, Australia, Canada and the United States; *Oryctocephalus* has been reported in the United States, Asia, South America, and Europe; *Bathyuriscus* is found in the northeastern United States and England; and *Elrathina* is found in Greenland, the United States and Canada. Brachiopods are also an important group found in the Chiuharruita Hill, and are represented by the genera *Acrothele*, found also in Europe, Asia, North America,

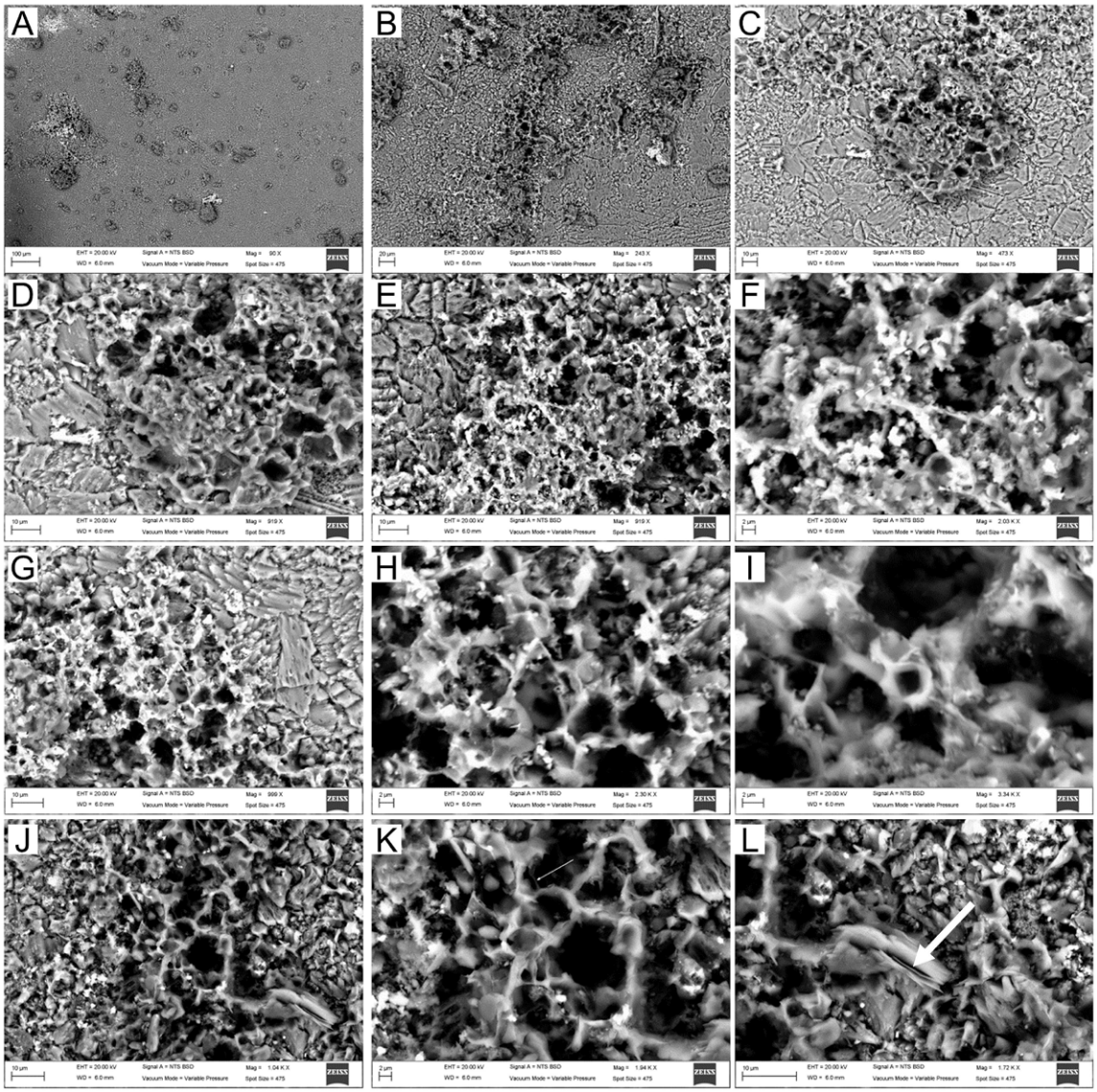

Figure 14. SEM photographs of reticulated structures within the rock matrix (outside the oncolitic structure). A, B, C, D. Incremental magnifications of reticulated structures show the overall circular shape in cross section (A, C, D), and the contrasting difference in texture with the surrounding matrix (C). Although similar to structures in Fig. 14 (L–R), these display a reticulated texture but are similar in composition (Fig. S9 A–B). E, F, G, H. These reticulated structures often display thread-like filaments that are < 2 μm in diameter and make up the bulk of the structures in cross section. I, J, K, L. Tubular structures (I; ~2 μm in diameter) and clays (J, L) are also present within these reticulated structures.

Australia, and North Africa; the genus *Dictyonina* is found in North America, Asia, and Europe; the genus *Prototreta* is found in Europe, America, and Asia; and *Linnarssonia* is found in North America and Europe. These fossils give the Cambrian of Sonora a worldwide stratigraphic context.

Paleogeographic reconstructions of North America (Scotese, 2002) place the platform where this fauna developed in Sonora in the tropics during the Early Cambrian. This was open to the Iapetus Ocean, with large landmasses (Baltica, Siberia, Avalonia, and northern Gondwana) relatively close by and located more or less in the tropics as well. Ongoing work is dealing with whether Lower Cambrian oncolites developed under similar conditions along that stretch of the Iapetus coastal areas, under the premise that oncolite markers exist in many strata of the world, and that they can be useful when used together with index fossils and lithology. Oncolites are present in stratigraphic ages other than the Cambrian and thus are not index fossils, but ambiguous stratigraphic markers by themselves (Rezak, 1957). However, when other, well-known index fossils are present they result in useful stratigraphic markers for close geographical regions, which is the case with the Caborca-SJG correlation. Regardless of the similarity in morphology, Cambrian oncolites are known from China (Hicks and Rowland, 2009; Zhang *et al*., 2015), Australia (Youngs, 1978; Walter, 1972), Jordan (Shinaq and Bandel, 1992; Elicki *et al*., 2002), Spain (Álvaro *et al*., 2000; Perejón *et al*., 2012), Antarctica (Rees *et al*., 1989), Argentina (Bordonaro, 2003; Gomez *et al*., 2007), Iran (Bayet-Goll *et al*., 2014), and Canada (Powell *et al*., 2006), which highlights the expansion of oncolites in the Cambrian as a global phenomena, with implications for paleoenvironmental and geobiological significance.

Localities from the USA are particularly important for correlations with the Chihuarruita Hill given their proximity and the extension of Cambrian outcrops to the south. The SW USA shares a lot in common with rocks and fossils from Sonora. Oncolites from Nevada, California, and Arizona (Johnson, 1952; Hose, 1961; Halley, 1975; Gilbert and Donovan, 1982; Rees, 1986) have particular characteristics according to their geographical location, particularly size, shape and color, which implies similar lithology and diagenesis. They tend to be darker than the matrix, can occur in hematizied horizons, their size ranges in ~20–50 mm, and most are nucleated and have concentric lamination. Some have been recovered from fine-grained carbonate rocks in the Chambless Formation and the Lower Cambrian Mule Spring Limestone, Nevada, USA, which have similar color, size, shape, style of lamination and depositional style than those from Caborca and SJG. In California, the Thimble Limestone Member of the Carrara Fm. (Palmer and Halley, 1979) bears *Bristolia bristolensis* and *Olenellus* sp. fragments and can thus be correlated with the oncolite-bearing Buelna Formation. Other index fossils found in SJG, such as molluscs *Hyolithes* and *Haplophrentis* and sponge-like spicules of *Chancelloria* and *Diagoniella*, are also found in the SW USA (Levi-Setti, 1995; Nardin *et al*., 2009; Cuen *et al*., 2013). The correlation between the Chihuarruita Hill and the Caborca region can be conceived as an extension of southern, Cambrian marine environments of Laurentia.

6. Conclusions

The overall geology of Chihuarruita Hill, the fossil content of the succession, and the composition of the rocks and their components is interpreted as a shallow, marginal marine carbonate platform, perhaps with a protected, back reef lagoon-type of setting, which is consistent with the studies by Cuen *et al*. (2016). Sand banks could have formed, given the intercalations with storm-deposited sandstones. Warm temperatures are thought to have enhanced carbonate deposition in waters with normal salinity (~3.5 %) and a steady source of Ca^{2+} and carbonate ions. The oncolites of SJG, are visually abundant in one rock unit of the Buelna Formation, but are known from northern localities in Sonora, and are similar to Cambrian oncolites from SW USA. They were important components of a larger biotic association in ecosystems that covered hundreds of square kilometers in the southern shores of Laurentia. Abundant skeletal grains in the limestone matrix and within oncolites depict a diverse fauna of a mature ecosystem with well established trophic chains. The absence of complete bodies of animals in the oncolitic limestone may indicate that the sediment was reworked in high energy, wave environment, where perhaps living metazoans were absent most of the time. Perhaps less metazoan grazing occurred in that area of the carbonate bank, allowing the oncolites to attain large diameters (44 mm). They formed clast-supported conglomerates in coastal facies of shallow marine environments through active nucleation around skeletal grains, promoted by microbial growth and carbonate precipitation. Microscopic features that resemble biological remains, such as coherent filamentous biofilms that are found within the oncolites, are consistent with a biological origin of the structures.

Trilobites, brachiopods, eocrinoids, sponges (hexactinellid) and molluscs (hyolitids) are found in strata that represent tenths of millions of years of deposition. Some index fossils (*e.g*. *Bristolia* sp., *Olenellus* sp.) indicate an age of ~510 Ma. The overall geology of the Chiuharruita Hill depicts a coastal paleoenvironment, with clastic shores and a carbonate, off-shore platform. The amount of carbonate suggests tropical, warm and well oxygenated waters (Cuen *et al*., 2016), and clastic sediments represent offshore platform environments. The oncolites themselves and the associated fauna, especially trilobites and ichnofossils, suggest a continental-scale continuum faunistic province in this part of North America. Further studies of Cambrian oncolites around the world could provide a better view of their extension, paleogeographical distribution, and role in ecology and evolution.

Acknowledgments

Research was funded by CONACyT grant No.165826, UNAM-DGAPA-PAPIIT grant No. IN101512 and ECOS FRANCIA-MEXICO grant No. M13-U01. We thank Kathleen B. Pigg (ASU), Teresa Pi Puig, Laura Luna González, Enoch Ortiz Montejo, Iris Suárez Quijada, Jaime Díaz Ortega, Rafael López Martínez, Margarita Reyes Salas, Sonia Ángeles García, Consuelo Macias Romo, Sergio Cevallos-Ferriz, Leticia Alba Aldave, and Fernando Nuñez Useche (Instituto de Geología, UNAM), David F. Blake (NASA-JPL), Chris Mavris (UCL), José Manuel Saniger Blesa and José Guadalupe Bañuelos (Laboratorio Universitario de Caracterización Espectroscópica - LUCE; Centro de Ciencias Aplicadas y Desarrollo Tecnológico - CCADET, UNAM), and Adriana Espino del Castillo (Rotoplas) for their contributions to this work. We thank Alberto Blanco Piñón and an anonymous reviewer for their useful comments. FCR acknowledges the Posgrado en Biocencias (DICTUS-UNISON) for providing facilities to carry out research aided with financial and technical support from CONACyT project No. 205981.

References

Almazán-Vázquez, E., 1989, El Cámbrico-Ordovícico de Arivechi, en la región centro-oriental del estado de Sonora: Revista del Instituto de Geología, Universidad Nacional Autónoma de México, 8(1), 58–66.

Alshuaibi, A., Duane, M.J., Mahmoud, H., 2012, Microbial-Activated Sediment Traps Associated with Oncolite Formation Along a Peritidal Beach, Northern Arabian (Persian) Gulf, Kuwait: Geomicrobiology Journal, 29(8), 679–696.

Álvaro, J.J., Vennin, E., Moreno-Eiris, E., Perejón, A., Bechstädt, T., 2000, Sedimentary patterns across the Lower–Middle Cambrian transition in the Esla nappe (Cantabrian Mountains, northern Spain): Sedimentary Geology, 137, 43–61.

Baldis, B.A.J., Bordonaro, O.L., 1981, Vinculación entre el Cámbrico del noroeste de México y la Precoordillera Argentina, en Porto Alegre, Brasil, II Congreso Latinoamericano de Paleontología, Annals. 1–10.

Balson, P.S., Taylor, P.D., 1982, Palaeobiology and systematics of large cyclostome bryozoans from the Pliocene Coralline Crag of Suffolk: Palaeontology, 25, 529–554.

Bauld, J., 1981, Geobiological role of cyanobacterial mats in sedimentary environments: production and preservation of organic matter: BMR Journal of Australian Geology and Geophysics, 6, 307–317.

Bayet-Goll, A., Geyer, G., Wilmsen, M., Mahboubi, A., Reza, S., Harami M., 2014, Facies architecture, depositional environments, and sequence stratigraphy of the Middle Cambrian Fasham and Deh-Sufiyan Formations in the central Alborz, Iran: Facies, 60(3), 815–841.

Beraldi-Campesi, H., Mann, D.G., Cevallos-Ferriz, S.R.S., 2015, Life cycle of 70 Ma-old non-marine pennate diatoms: Cretaceous Research, 56, 662–672.

Bish, D.L., Blake, D., Sarrazin, P., Treiman, A.H., Hoehler, T., Hausrath, E.M., Midtkandal, I., Steele, A., 2007, Field XRD/XRF mineral analysis by the MSL CheMin instrument: LPSC XXXVIII, Abstract #1163.

Bordonaro, O.L., 2003, Evolución paleoambiental y paleogeográfica de la cuenca cámbrica de la Precordillera argentina: Revista de la Asociación Geológica Argentina, 58(3), 329–346.

Buick, R., 1990, Microfossil recognition in Archean rocks; an appraisal of spheroids and filaments from a 3500 m.y. old chert-barite unit at North Pole, Western Australia: PALAIOS, 5, 441–459.

Buitrón-Sánchez, B.E., Vachard, D., Almazán-Vázquez, E., Palafox, J.J., 2012, A Carboniferous to lower Permian cratonic sequence exposed in El Tule hills, northeastern Sonora, Mexico: Revista Mexicana de Ciencias Geológicas, 29(1), 39–62.

Buitrón-Sánchez, B., Corona-González, N., Cuen, F.J., Palafox-Reyes, J.J., Ramírez-Guerrero, G., 2016, Icnofósiles del Cámbrico Inferior de San José de Gracia, Sonora: Paleontología Mexicana, 5(1), 33–40.

Cooper, G.A., Arellano, A., Jhonson, J., Okulitch J., Stoyanow, A. Lochman, C., 1952, Cambrian stratigraphy and paleontology near Caborca, northwestern Sonora, México: Smithsonian Miscellaneous Collections, 119(1), 1–178.

Cuen, F.J., Beresi, M.S., Montijo, A., Buitrón, B.E., Minjarez, I., De la O, M., 2013, Chancelloriida Walcott, 1920 y Reticulosa Reid, 1958 del Cámbrico medio de San José de Gracia, Sonora, México: Boletín de la Sociedad Geológica Mexicana, 65(3), 581–590.

Cuen, F.J., Valdez, J.E., Buitrón, B.E., Monreal-Saavedra, R., Sundberg, F., Montijo-González, A., Minjarez-Sosa, I., 2016, Cambrian stratigraphy of San José de Gracia, Sonora, México: El Gavilán Formation, a new middle Cambrian lithostratigraphic unit of open shelf environment: Boletín de la Sociedad Geológica Mexicana, 68(3), 429–441.

Debrenne, F., Gandin, A., Rowland, S.M., 1989, Lower Cambrian bioconstructions in northwestern Mexico (Sonora) - Depositional setting, paleoecology and systematics of archaeocyaths: Geobios, 22(2), 137–195.

Dunlop, J.S.R., Muir, M.D., Milne, V.A., Groves, D.I., 1978, A new microfossil assemblage from the Archaean of Western Australia: Nature, 274, 676–678.

Dupraz, C., Visscher, P.T., 2005, Microbial lithification in marine stromatolites and hypersaline mat: Trends in Microbiology, 13, 429–438.

Elicki, O., Schneider, J., Shinaq, R., 2002, Prominent facies from the Lower/Middle Cambrian of the Dead Sea area (Jordan) and their palaeodepositional significance: Bulletin de la Société Géologique de France, 173, 547–552.

Flügel, E., 2004, Microfacies of Carbonate Rocks. Analysis, Interpretation and Application: Springer-Verlag, Berlin, 976 pp.

Garcia-Pichel, F., Ramirez-Reinat, E., Gao, Q., 2010, Microbial excavation of solid carbonates powered by P-type ATPase-mediated transcellular Ca^{2+} transport: Proceedings of the National Academy of Sciences, 107, 21749–21754.

Gilbert, M.C., Donovan, R.N. (eds), 1982, Geology of the Eastern Wichita Mountains, Southwestern Oklahoma: Oklahoma Geological Survey Guidebook, 21, 160 pp.

Gomez, F.J., Ogle, N., Astini, R.A., Kalin, R.M., 2007, Paleoenvironmental and carbon–oxygen isotope record of Middle Cambrian Carbonates (La Laja Formation) in the Argentine Precordillera: Journal of Sedimentary Research, 77, 826–842.

Halley, R.G., 1975, Peritidal lithologies of Cambrian carbonate islands, Carrara Foramtion southern Great Basin, *in* Ginsburg, R.N. (ed.): Tidal Deposits, Springer, Berlin, 279–288.

Henderson, J.B., 1975, Archean Stromatolites in the Northern Slave Province, Northwest Territories, Canada: Canadian Journal of Earth Sciences, 12(9), 1619–1630.

Hicks, M., Rowland, S.M., 2009, Early Cambrian microbial reefs, archaeocyathan inter-reef communities, and associated facies of the Yangtze Platform: Palaeogeography, Palaeoclimatology, Palaeoecology, 281(1–2), 137–153.

Hillmer, G., Scholz, J., Wolf-Christian, D., 1996, Two types of bryozoan nodules from the Gulf of Aqaba, Red Sea, *in* Gordon, D.P., Smith, A.M., Grant-Mackie, J.A. (eds.): Bryozoans in Space and Time, NIWA, Wellington, 125–130.

Hose, R.K., 1961, Physical characteristics of Upper Cambrian stromatolites in western Utah: US Geological Survey, Professional Paper, 424-D, Washington, USA, 245–248.

Johnson, J.H., 1952, *Girvanella*, *in* Cooper, G.A., Arellano, A.R.V., Johnson, J. H., Okulitch, V.J., Stoyanow, A., Lochman, C. (eds.). Cambrian stratigraphy and paleontology near Caborca, northwestern Sonora, Mexico: Smithsonian Miscellaneous Collections, 119(1), 24–26.

Kah, L.C., Riding, R., 2007, Mesoproterozoic carbon dioxide levels inferred from calcified cyanobacteria: Geology, 35, 799–802.

King, R.E., 1940, Pre-Tertiary history of the Sierra Madre Occidental of Sonora and Chihuahua and some adjacent parts of central Sonora, México: Sexto Congreso Científico, Proceedings, 1, 217–222.

Knoll, A.H., Swett, K., Burkhardt, E., 1989, Paleoenvironmental Distribution of Microfossils and Stromatolites in the Upper Proterozoic Backlundtoppen Formation, Spitsbergen: Journal of Paleontology, 63(2), 129–145.

Laval, B., Cady, S.L., Pollack, J.C., McKay, C.P., Bird, J.S., Grotzinger, J.P., Ford, D.C., Bohm, H.R., 2000, Modern freshwater microbialite analogues for ancient dendritic reef structures: Nature, 407(6804), 626–629.

Levi-Setti, R., 1995, Trilobites: The University of Chicago Press, 2nd ed., 342 pp.

Lowe, D.R., 1983, Restricted shallow-water sedimentation of Early Archean stromatolitic and evaporitic strata of the Strelley Pool Chert, Pilbara block, Western Australia: Precambrian Research, 19, 239–283.

McMenamin, N.M., 1985, Basal Cambrian small shelly fossils from La Ciénega Fm. NW, Sonora: Journal of Paleontology, 59, 1414–1425.

McMenamin, N.M., 1987, Lower Cambrian zonation and correlation of the Puerto Blanco, Fm. Sonora: Journal of Paleontology, 4, 738–749.

Nardin, E., Almazán-Vázquez, E., Buitrón-Sánchez, B.E., 2009, First report of *Gogia* (Eocrinoidea, Echinodermata) from de Early-Middle Cambrian of Sonora (México), with bioestratigraphical and palaecological comments: Geobios, 42, 233–242.

Nicholson, H.A., Etheridge, R., 1878, Silurian fossils of the Girvan District in Ayrshire. With special reference to those contained in the "Grey Collection": William Blackwood and Sons, Fasciculus 1, Edinburgh and London, 135 pp.

Palmer, A.R., Halley, R.B., 1979, Physical stratigraphy and trilobite biostratigraphy of the Carrara Formation (Lower and Middle Cambrian) in the southern Great Basin: US Geological Survey, Professional Paper, 1047 pp.

Perejón, A., Moreno-Eiris, E., Bechstädt, T., Menéndez, S., Rodríguez-Martínez, M., 2012, New Bilbilian (Early Cambrian) archaeocyath-rich thrombolitic microbialite from the Láncara Formation (Cantabrian Mts., northern Spain): Journal of Iberian Geology, 38, 313–330.

Peryt, T.M., 1981, Phanerozoic oncoids: an overview: Facies, 4, 197–214.

Pickford, M., Senut, B., Hipondoka, M., Person, A., Segalen, L., Plet, C., Jousse, H., Mein, P., Guerin, C., Morales, J., Mourer-Chauvire, C., 2009, Mio-Plio-Pleistocene geology and palaeobiology of Etosha Pan, Namibia: Communications of the Geological Survey of Namibia, 14, 95–139.

Planavsky, N., Reid, P., Lyons, W., Myshrall, L., Visscher, P., 2009, Formation and diagenesis of modern marine calcified cyanobacteria: Geobiology, 7, 566–576.

Powell, W.G., Johnston, P.A., Collom, C.J., Johnston, K.J., 2006, Middle Cambrian brine seeps on the Kicking Horse Rim and their relationship to talc and magnesite mineralization and associated dolomitization, British Columbia, Canada: Economic Geology, 101, 431–451.

Rees, M.N., 1986, A fault-controlled trough through a carbonate platform: The Middle Cambrian House Range embayment: Geological Society of America Bulletin, 97, 1054–1069.

Rees, M.N., Pratt, B.R., Rowells, A.J., 1989, Early Cambrian reefs, reef complexes, and associated lithofacies of the Shackleton Limestone, Transantarctic Mountains: Sedimentology, 36, 341–361.

Reimer, T.O., 1975, Paleogeographic significance of the oldest known oolite pebbles in the Archaean Swaziland Supergroup (South Africa): Sedimentary Geology, 14(2), 123–133.

Rezak, R., 1957, *Girvanella* not a guide to the cambrian: Bulletin of the Geological Society of America, 68, 1411–1412.

Rider, J., Enrico, R., 1979, Structural and functional adaptations of mobile anascan ectoproct colonies (ectoproctaliths), *in* Larwood, G.P., Abbott, M.B. (eds.): Advances in Bryozoology Systematics Association, Special Volume 13, Academic Press, London, 297–319.

Riding, R., 1975, *Girvanella* and other algae as depth indicators: Lethaia, 8, 173–179.

Riding, R., 1977, Calcified *Plectonema* (blue–green algae), a recent example of *Girvanella* from Aldabra Atoll: Palaeontology, 20, 33–46.

Riding, R., 2006, Cyanobacterial calcification, carbon dioxide concentrating mechanisms, and Proterozoic–Cambrian changes in atmospheric composition: Geobiology, 4, 299–316.

Riva, J., Ketner, K.B., 1989, Ordovician graptolites from the northern Sierra de Cobachi, Sonora, Mexico: Transactions of the Royal Society of Edinburgh, Earth Sciences, 80, 71–90.

Rivera-Carranco, E., 1988a, Condiciones Paleoambientales de depósito de las Formaciones Cámbricas del área de Caborca, Sonora: Revista Mexicana de Ciencias Geológicas, 7(1), 22–27.

Rivera-Carranco, E., 1988b, Génesis de la Formación Proveedora (Cámbrico Inferior) del área de Caborca, Sonora: noroccidental: Revista Mexicana de Ciencias Geológicas, 7(2), 163–167.

Robison, R.A., 1965, Middle Cambrian Eocrinoids from Western North America: Journal of Paleontology, 39, 355–364.

Sander, S.G., Koschinsky, A., 2011, Metal flux from hydrothermal vents increased by organic complexation: Nature Geoscience, 4(3), 145–150.

Scholz, J., 2000, A field theory of bryozoans, microbial mats and sediment surfaces: Proceedings of the Senckenberg Nature Research, Waldemar Kramer, Gesellscaft, Frankfurt, 552, 1–193.

Schopf, J.W., 1993, Microfossils of the early Archean Apex Chert—new evidence of the antiquity of life: Science, 260, 640–646.

Schopf, J.W., Kudryavtsev, A.B., 2009, Confocal laser scanning microscopy and Raman imagery of ancient microscopic fossils: Precambrian Research, 173, 39–49.

Scotese, C.R., 2002, http://www.scotese.com, (PALEOMAP website), *viewed in* September, 2016.

Shepard, R.N., Sumner, D.Y., 2010, Undirected motility of cyanobacteria produces reticulate mats: Geobiology, 8, 179–190.

Shinaq, R., Bandel, K., 1992, Microfacies of Cambrian Limestones in Jordan: Facies, 27(1), 263–283.

Sim, M.S., Liang, B. Petroff, A.P., Evans, A., Klepac-Ceraj, V., Flannery, D.T., Walter, M.R., Bosak, T., 2012, Oxygen-Dependent Morphogenesis of Modern Clumped Photosynthetic Mats and Implications for the Archean Stromatolite Record: Geosciences, 2, 235–259.

Sprinkle, J., 1973, Morphology and evolution of blastozoan echinoderms: Harvard University, Museum of Comparative Zoology Special Publication, 1–284.

Stewart, J.H., McMenamin, A.S., Morales-Ramirez, J.M., 1984, Upper Proterozoic and Cambrian Rocks in the Caborca Region, Sonora, México. Physical Stratigraphy, Biostratigraphy, Paleocurrent Studies and Regional relations: US Geological Survey Professional Paper 1309, 36 pp.

Stewart, J.H., Amaya-Martínez, R., Palmer, A.R., 2002, Neoproterozoic and Cambrian strata of Sonora, México: Rodinian supercontinent to Laurentian Cordilleran margin, *in* Barth, A. (ed.), Crustal evolution in the southwest USA: Geological Society of America Special Paper 365, 5–48.

Theis, T.L., Singer, P.C., 1974, Complexation of iron(III) by organic matter and its effect on iron(II) oxygenation: Environmental Sciences and Technology, 8, 569–572.

Wade, B.D., Garcia-Pichel, F., 2003, Evaluation of DNA Extraction Methods for Molecular Analyses of Microbial Communities in Modern Calcareous Microbialites: Geomicrobiology Journal, 20(6), 549–561.

Walter, M.R., 1972, Stromatolites and the biostratigraphy of the Australian Precambrian and Cambrian: Special Papers in Palaeontology, 11, 1–190.

Wilmeth, D.T., Corsetti, F.A., Bisenic, N., Dornbos, S.Q., Oji, T., Gonchigdorj, S., 2015, Punctuated growth of microbial cones within Early Cambrian oncoids, Bayan Gol Formation, Western Mongolia: Palaios, 30(12), 836–845.

Winsborough, B.M., Seeler, J.S., Golubic, S., Folk, R.L., Maguire, Jr. B., 1994, Recent fresh-water lacustrine stromatolites, stromatolitic mats and oncoids from northeastern Mexico, *in* Bertrand-Sarfati, J., Monty, C.L.V. (eds.) Phanerozoic Stromatolites II. The Netherlands: Kluwer Academic Publishers, 71–100.

Wood, A., 1957, The type-species of the genus *Girvanella* (Calcareous algae): Palaeontology, 1(1), 22–28.

Youngs, B.C., 1978, The petrology and depositional environments of the Middle Cambrian Wirrealpa and Aroona Creek limestones (South Australia): Journal of Sedimentary Petrology, 48, 63–74.

Zhang, W., Shi, X., Jiang, G., Tang, D., Wang, X., 2015, Mass-occurrence of oncoids at the Cambrian Series 2–Series 3 transition: Implications for microbial resurgence following an Early Cambrian extinction: Gondwana Research, 28, 432–450.

Zonneveld, K.A.F., Versteegh, G.J.M., Kasten, S., Eglinton, T.I., Emeis, K.C., Huguet, C., Koch, B.P., De Lange, G.J., De Leeuw, J.W., Middelburg, J.J., Mollenhauer, G., Prahl, F.G., Rethemeyer, J., Wakeham, S.G., 2010, Selective preservation of organic matter in marine environments; processes and impact on the sedimentary record: Biogeosciences, 7, 483–511.

Manuscript received: May 6, 2018.
Corrected manuscript received: June 3, 2018.
Manuscript accepted: June 4, 2018.

Supplementary materials

Figure S1. Examples of fossils and ichnofossils from the Chihuarruita Hill in SJG. Their stratigraphical distribution is indicated in Fig. 2 of the main text. A. Cast of the trilobite *Elrathina antiqua* Palmer and Halley, 1979. B. Torax and pigidium of *E. antiqua*. C. Cranidia and torax of E. antiqua. D. *Pentagnostus* (*Meragostus*) *bonnerensis* (Resser, 1939) Naimark, 2012. E. Thorax and pygidium of the trilobite *Oryctocephalites walcotti*. F. Burrows of *Palaeophycus* isp. in oblique view. G. Galleries of *Skolithos* isp. in cross view. H. Plan view of *Arenicolites* isp. burrows. I. Galleries of *Thalassinoides* isp. J. Large *Skolithos* isp. gallery. K–L. Plan view of *Asterosoma* isp. burrows. M. Plan view of a *Skolithos* isp. gallery. N. Complete skeleton of a large *Elrathina antiqua*. O. Skeleton of the trilobite *Ptychagnostus praecurrens*. P. Oblique view of *Skolithos* isp. standing up from the eroded matrix. Q. *Arenicolites* isp. in vertical cross section.

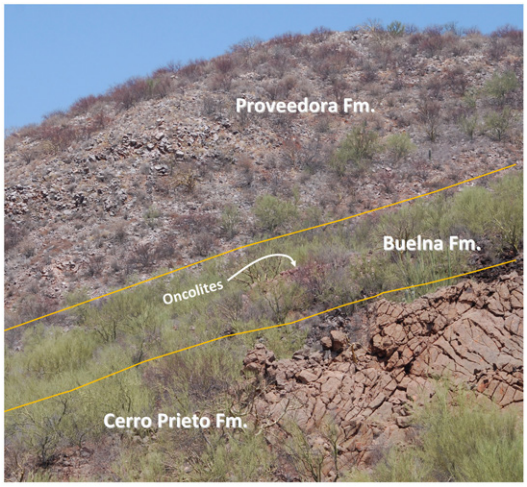

Figure S2. Field view of the Proveedora, Buelna, and Cerro Prieto formations. An oolitic block of the Cerro Prieto Fm. stands in the lower right, followed by inclined terrain of the Buelna Fm. that extends > 120 m before coming in contact with the Proveedora Fm. at its base. The massive oncolitic limestone unit can be seen close to the Buelna-Cerro Prieto contact.

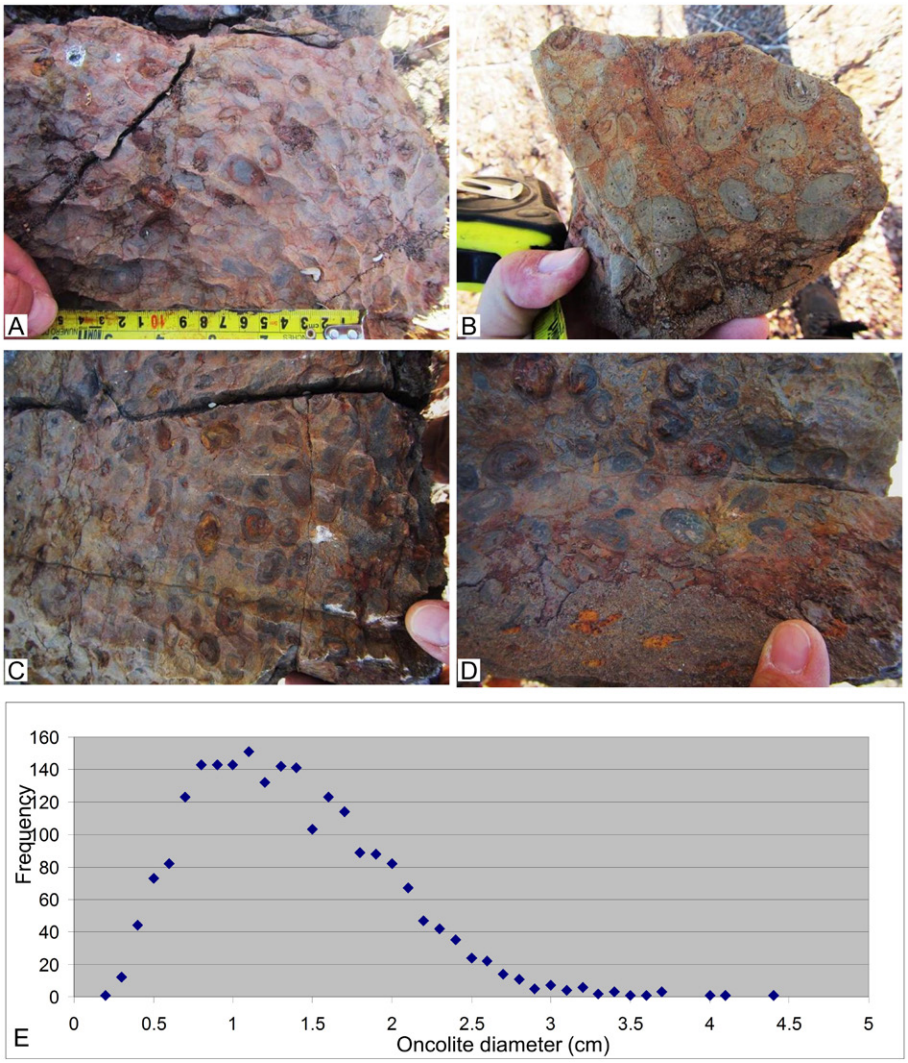

Figure S3. Field view of oncolites. A. Clast-supported oncolites. B. Matrix-supported oncolites. C. Graded oncolites. The base of the stratum is to the right and it grades up in size to the top (left). D. Oncolites in a packstone matrix, overlying a ferruginous sandstone bank. E. Frequency distribution of oncolite diameters (n = 2226).

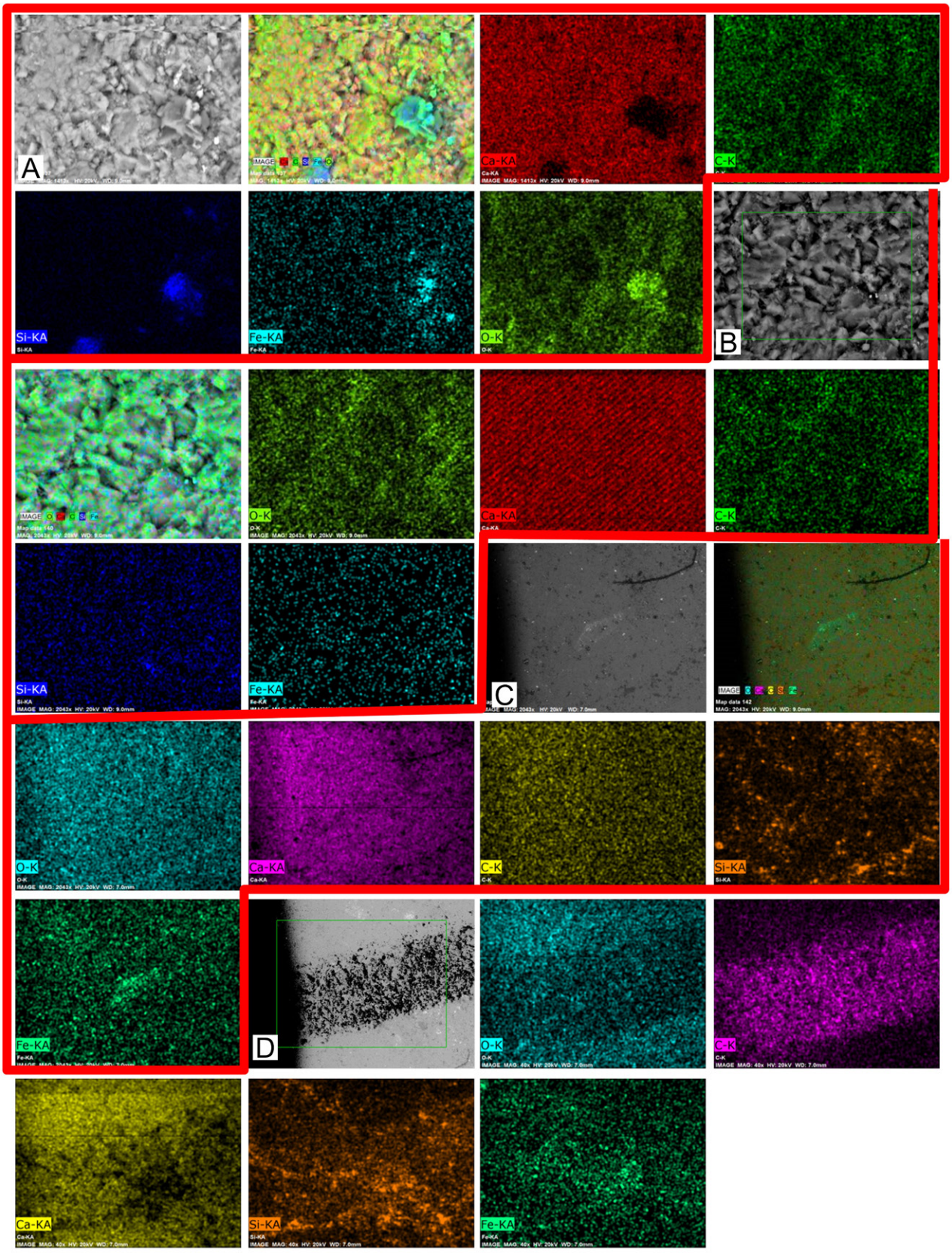

Figure S4. EDX spectra obtained with an electron microscope (see methods). Colors show the spectral composition of chemical elements. A. Silicified structures in the matrix of the rock between oncolites. B. Filament-like structures found in the matrix, outside an oncolite. C. Fe-rich structures in the rock matrix between the oncolites. D. Pencil strike on a clear portion (no skeletal or detrital fragments at the surface) of the limestone matrix to show the signal of graphite.

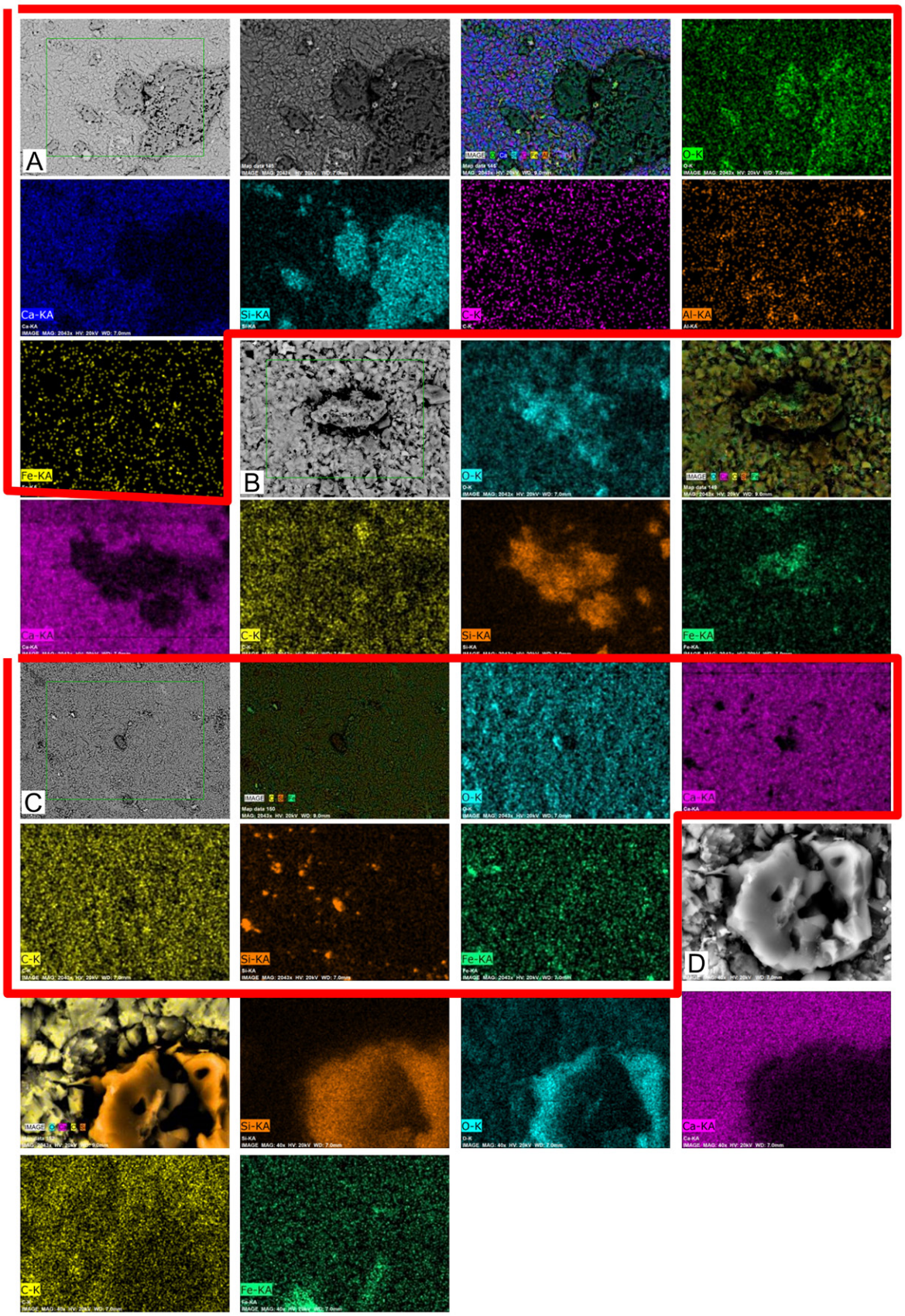

Figure S5. EDX spectra obtained with an electron microscope (see methods). Colors show the spectral composition of chemical elements. A. Silicified blobs found in the rock matrix between oncolites. B. Ellipsoidal structure rich in silica and iron, found in the rock matrix. C. General view of Si-rich and Fe-rich scattered objects shown in B. D. Close up of a silicified filamentous structure in cross section. Figure 14 L–R shows details of these structures.

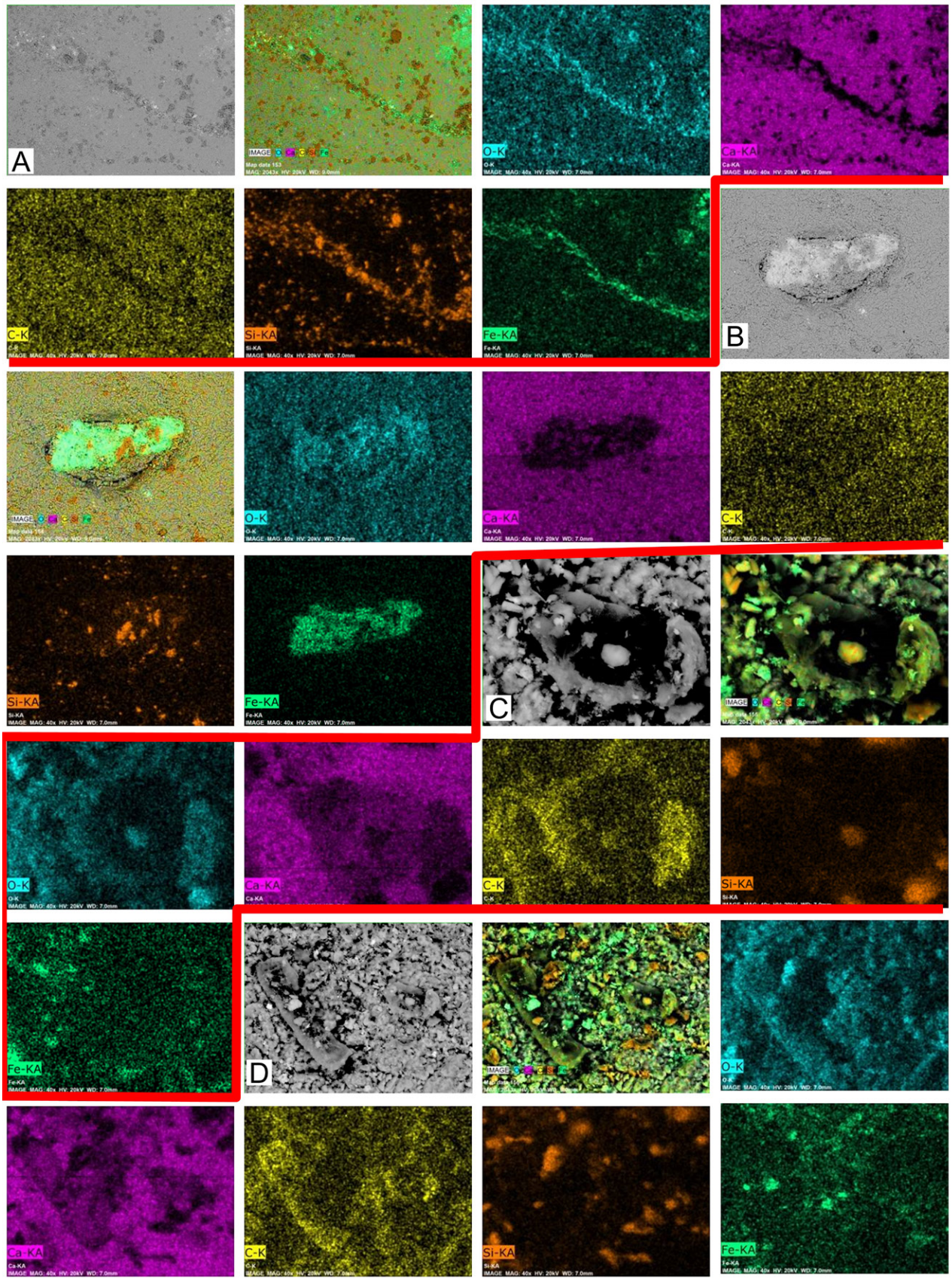

Figure S6. EDX spectra obtained with an electron microscope (see methods). Colors show the spectral composition of chemical elements. A. Section of an Fe-rich and Si-rich lamina of an oncolite, sandwiched between thicker calcitic laminae. B. Fe-rich structures within the oncolite lamination. C. Calcitic, filament-like structure in cross section, with a silicified nucleus. D. Carbonaceous structure loosely attached to the surface of the oncolitic matrix.

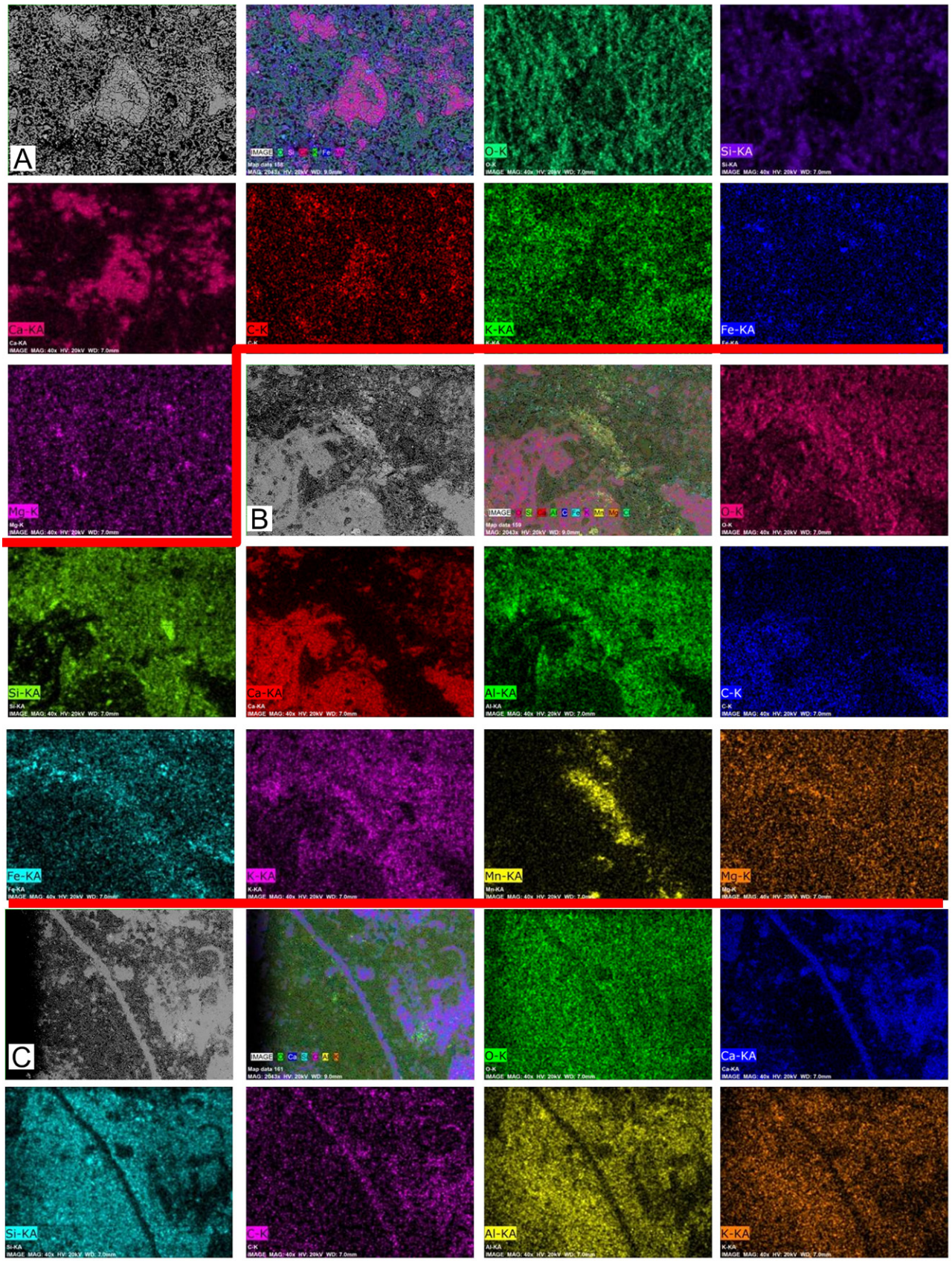

Figure S7. EDX spectra obtained with an electron microscope (see methods). Colors show the spectral composition of chemical elements. A. Ca-rich structures within a K-rich portion of the oncolitic matrix. B. Ca-rich skeletal particles within a portion of silicified matrix rich in Al and K. Note a Mn-rich particle at the center of the image. C. Calcitic skeletal grains embedded in a Si-Al-K-rich portion of the rock matrix.

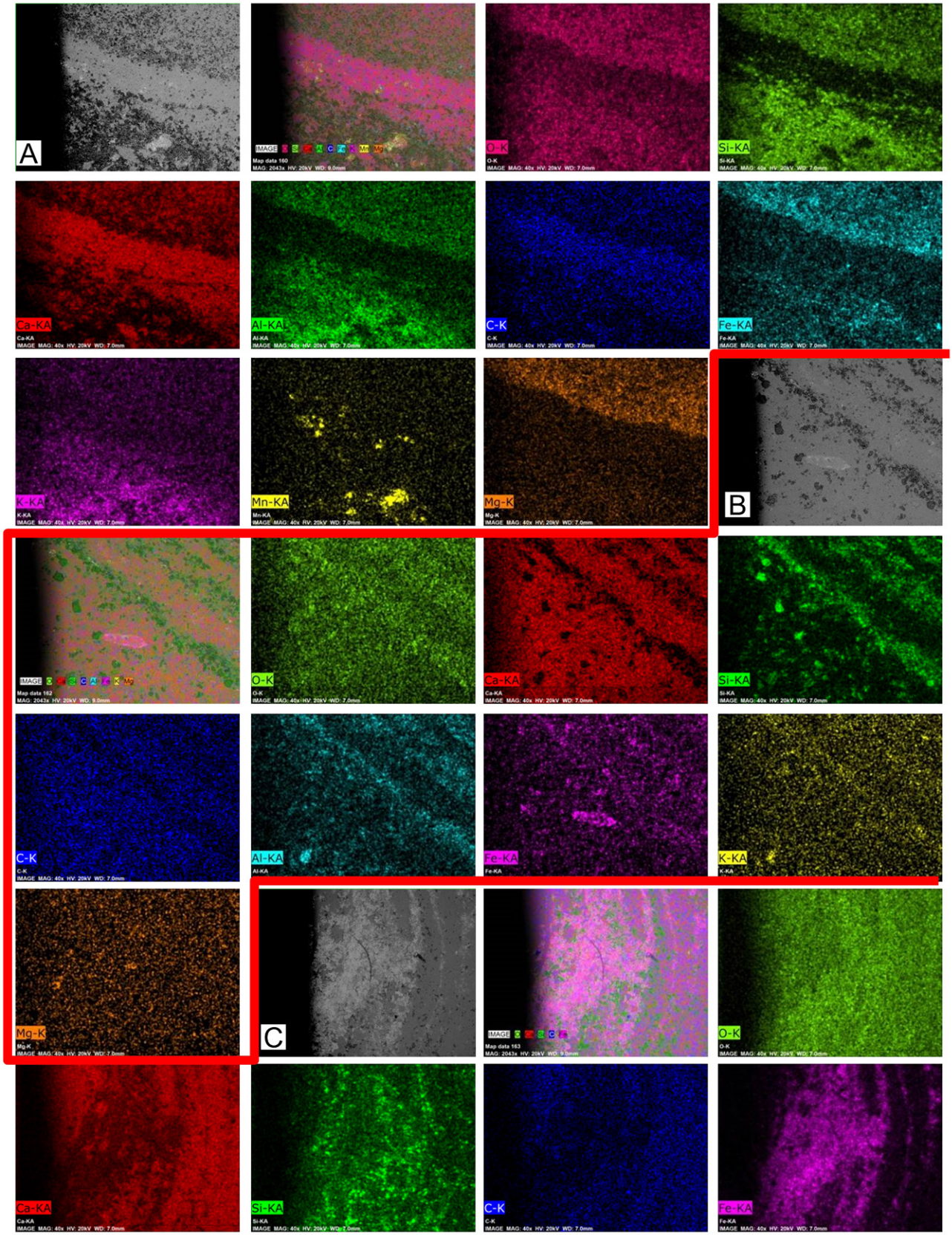

Figure S8. EDX spectra obtained with an electron microscope (see methods). Colors show the spectral composition of chemical elements. A. Oncolitic lamination showing calcitic laminae within a silicified portion of the oncolite, and scattered Mn-rich particles. B. Contrary to A, some lamination of the oncolites appeared rich in silica, and surrounded by a calcitic matrix. C. Fe-rich laminae of an oncolite surrounded by a calcitic matrix.

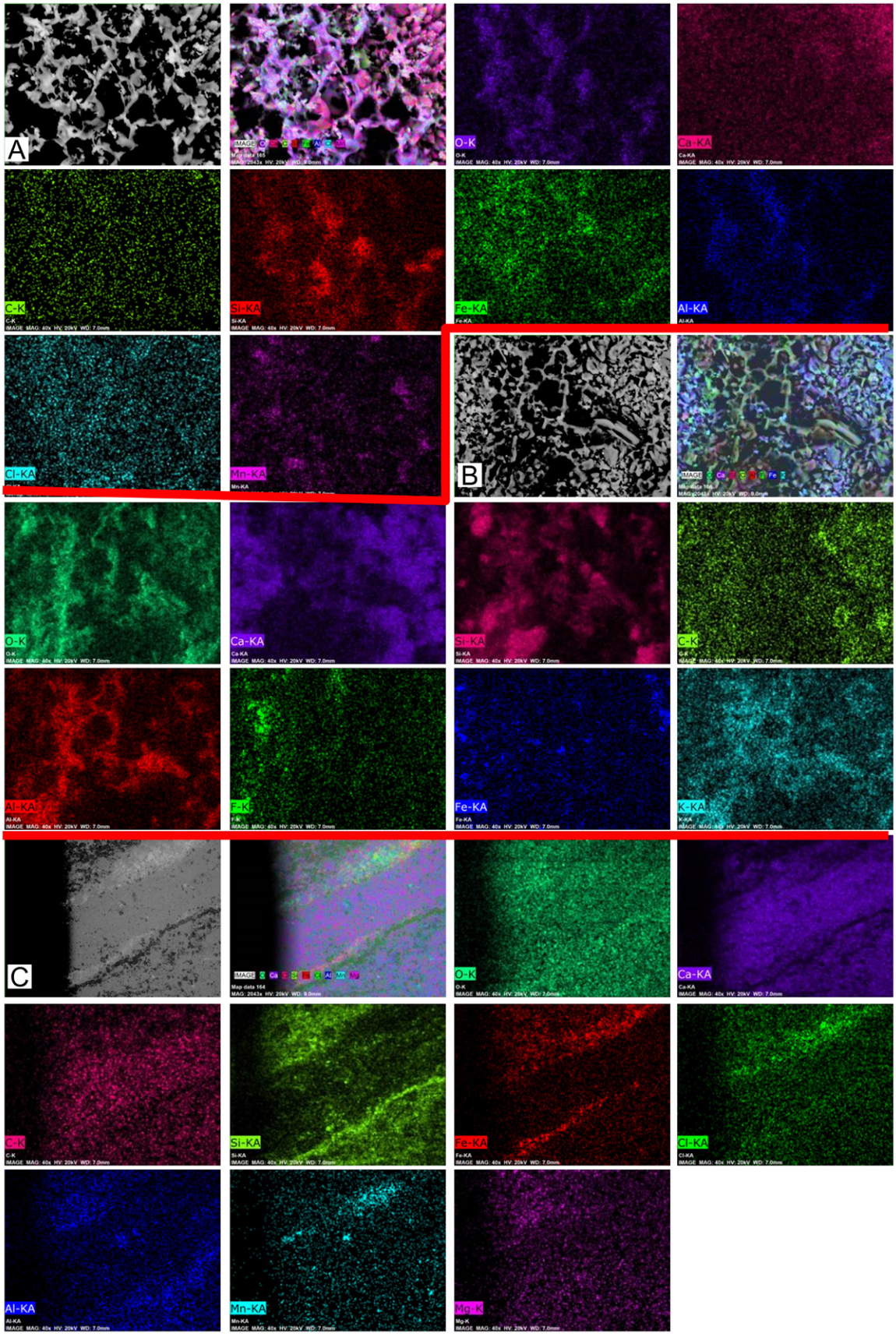

Figure S9. EDX spectra obtained from the oncolitic lamination. Colors show the spectral composition of chemical elements. A. Silicified reticulated structures within an oncolite. B. Another reticulated structure enriched in Al. C. Si- and Fe-rich lamination within an oncolite.

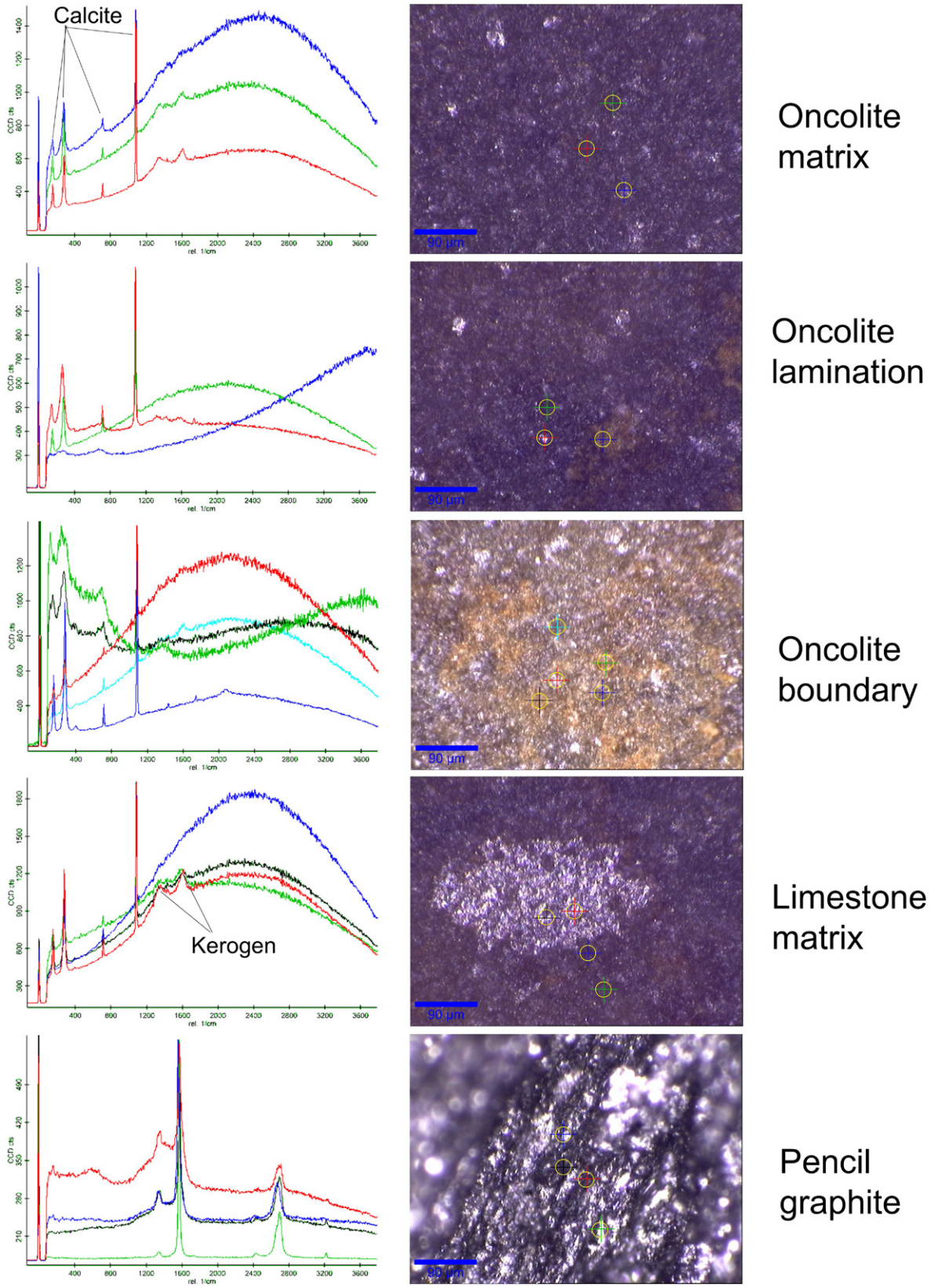

Figure S10. Raman spectra of different areas within the oncolite lamination, the limestone matrix, and pencil graphite to show the signal of kerogenous material within the rock samples. Colored circles on images indicate the measured points. Scale bars on images = 90 µm.

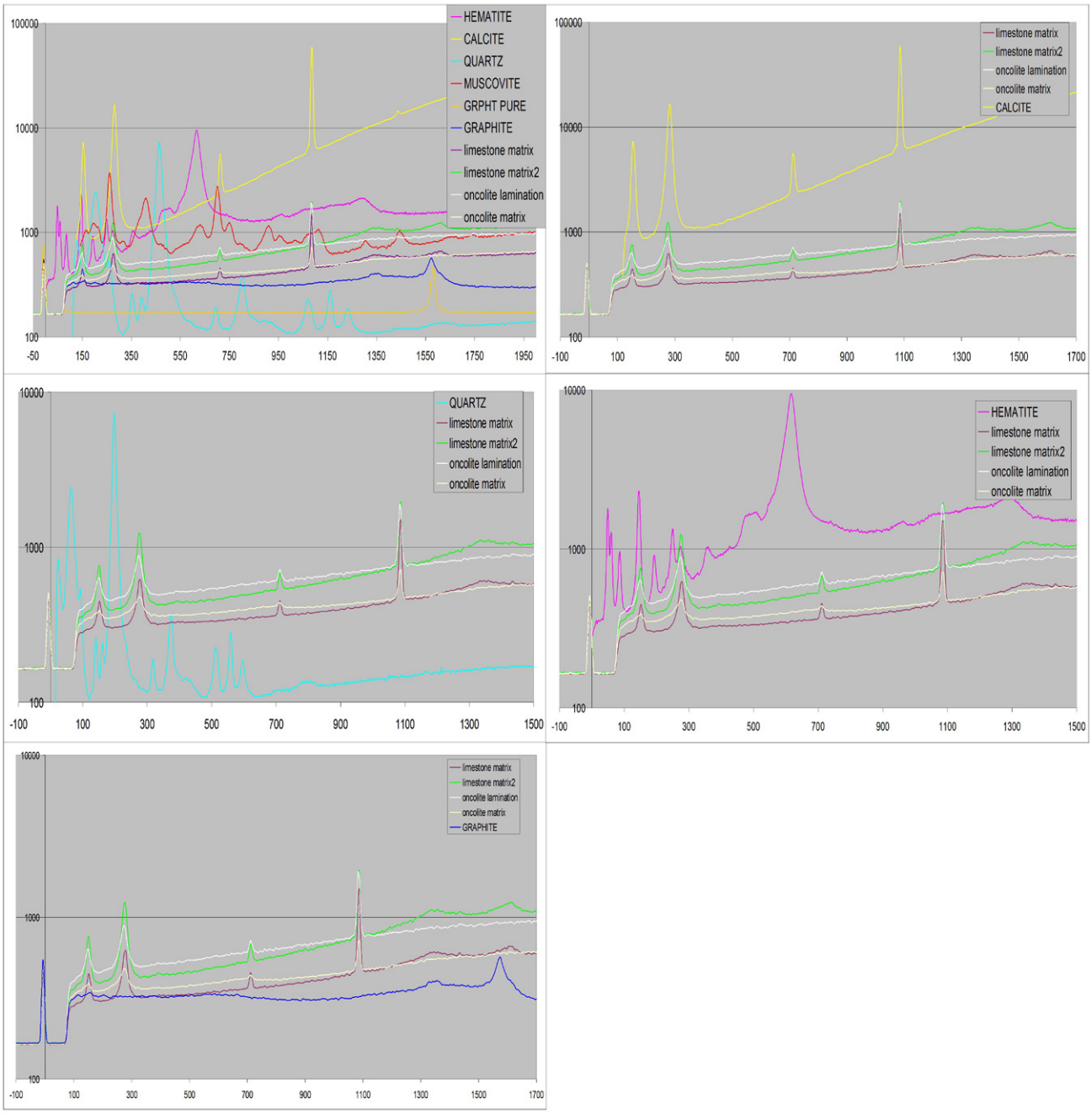

Figure S11. Raman spectra of standard minerals and samples from San José de Gracia. Standard curves *vs.* physical standard.

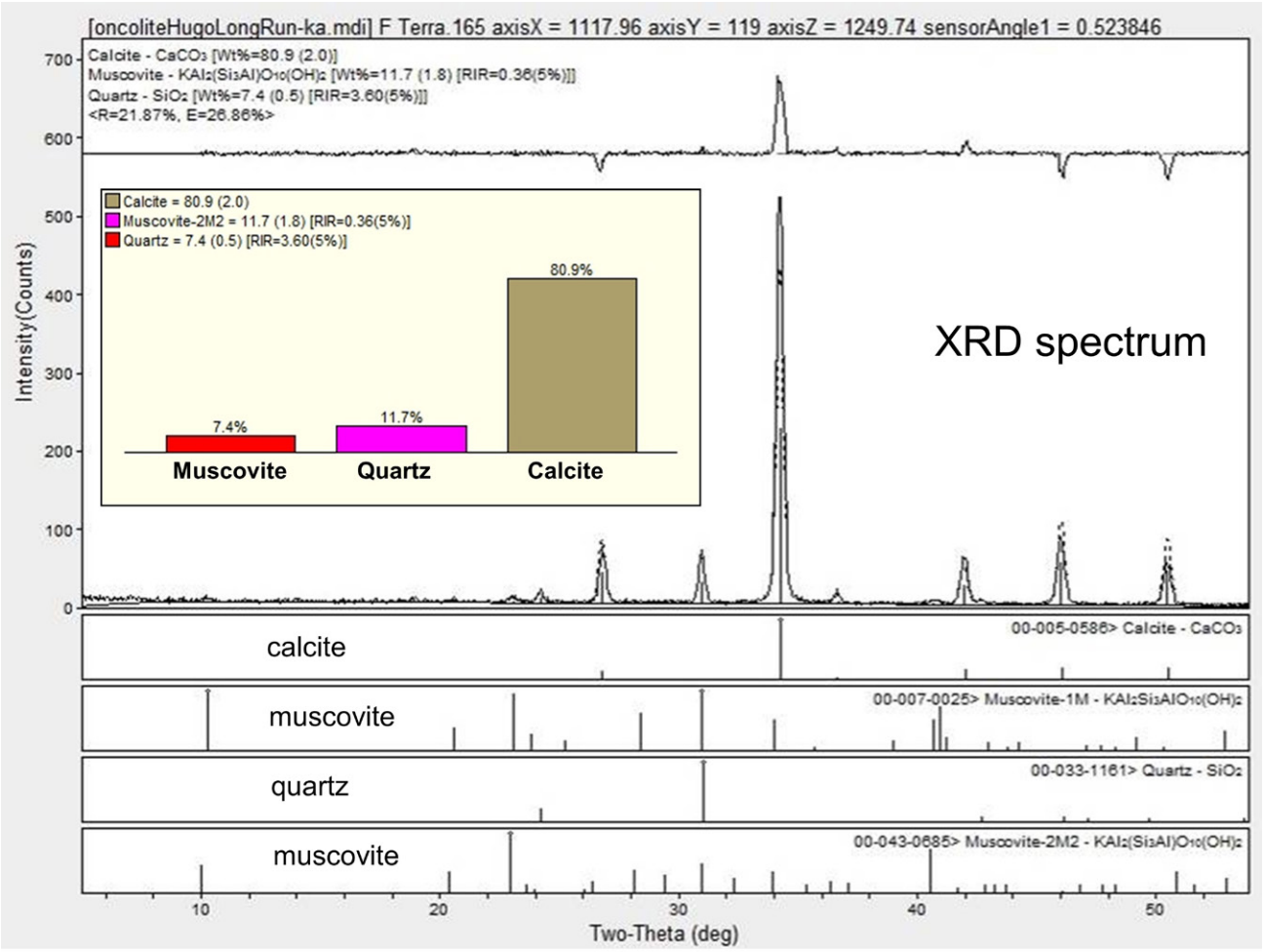

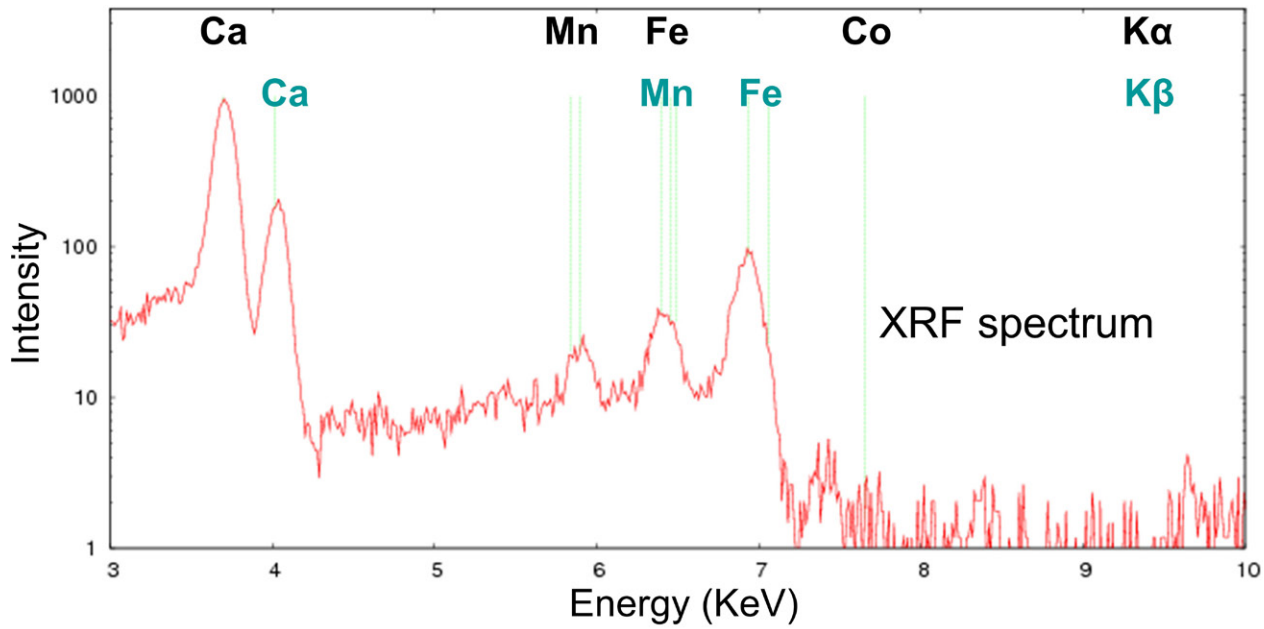

Figure S12. XRD and XRF analyses of a powdered oncolite. More than 80% is calcite, with minor amounts of quartz and muscovite. Ca, Mn, and Fe were present as impurities. XRF indicated the presence of Ca, Mn, Fe and Co.